

EQUI-VOCAL: Synthesizing Queries for Compositional Video Events from Limited User Interactions

Technical Report

Enhao Zhang¹, Maureen Daum¹, Dong He¹,
Brandon Haynes², Ranjay Krishna¹, and Magdalena Balazinska¹

¹University of Washington, {enhaoz, mdaum, donghe, ranjay, magda}@cs.washington.edu

²Microsoft Gray Systems Lab, brandon.haynes@microsoft.com

ABSTRACT

We introduce EQUI-VOCAL: a new system that automatically synthesizes queries over videos from limited user interactions. The user only provides a handful of positive and negative examples of what they are looking for. EQUI-VOCAL utilizes these initial examples and additional ones collected through active learning to efficiently synthesize complex user queries. Our approach enables users to find events without database expertise, with limited labeling effort, and without declarative specifications or sketches. Core to EQUI-VOCAL’s design is the use of spatio-temporal scene graphs in its data model and query language and a novel query synthesis approach that works on large and noisy video data. Our system outperforms two baseline systems—in terms of F1 score, synthesis time, and robustness to noise—and can flexibly synthesize complex queries that the baselines do not support.

1 INTRODUCTION

Video data is increasingly becoming a prized commodity. Inexpensive large-scale video storage and advances in machine learning and computer vision have propelled the use of large video datasets with new applications including drone analytics [75, 77], citywide traffic analytics [3, 27], civil engineering [5, 26], and many others [25, 53, 58, 67, 69]. Although video database management systems (VDBMSs) have recently re-emerged as an active research area to support these applications [4, 6, 18, 24, 40, 41, 50], existing systems fall short of supporting many use cases.

Consider a traffic analytics application: A traffic engineer may want to understand road hazards involving car and motorcycle interactions (e.g., motorcycles swerving abruptly in front of turning cars). Although many computer vision models exist that detect common objects (e.g., “cars” and “motorcycles”) [78] and relate objects spatially (e.g., “bottom of”, “left of”, “near”) [13], a specific classifier that identifies “a motorcycle swerving in front of a car, while the car is turning at an intersection” is unlikely to exist [80, 82]. Worse, training one would require many hours of user effort in labeling for a single query. Given the relative rarity of most interesting events, finding sufficient positive instances further exacerbates these labeling requirements. In our example, there will be many instances of cars and motorcycles in intersections. Only rarely would a motorcycle swerve in front of a turning car.

Assuming that we can run existing computer vision models on videos to identify objects, extract attributes, and reason about their pairwise relationships, some recent video data management systems support users by providing an interface to express a declarative query as a composition of extracted information [8, 12, 15, 24, 50, 55, 80]. For example, a user might be able

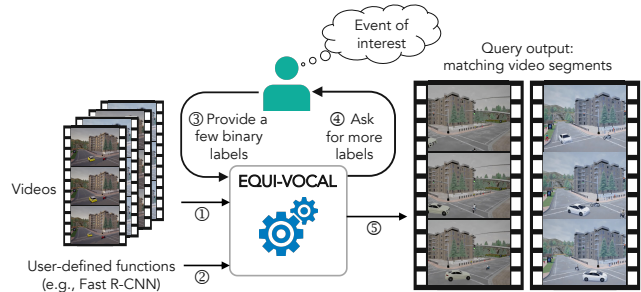


Figure 1: Given ① a video dataset, ② user-defined functions that extract semantic information from videos, and ③ a few user-provided labels, EQUI-VOCAL synthesizes a query to find instances of an event of interest. It iteratively ④ asks the user for more labels to reduce its uncertainty. Once synthesized, it ⑤ executes the query to return matching events on unseen videos.

to query for an event using a specification that searches for video clips containing car and motorcycle objects, and specifying their desired relationships (near then front_of, etc.). These systems expect users to possess a level of database expertise to be able to express such queries. Additionally, real-world events can be difficult to express declaratively—even for experts. For example, there are multiple ways to express our sample query. The best way depends on the data (e.g., in a given video, motorcycles may be swerving from outside the frame, as illustrated in Figure 2, discussed later). Other similar systems ask users to sketch their events [11, 15]; this is equally challenging for the same reason: an event of interest may deviate from the exact user-provided sketch.

In this paper, we present EQUI-VOCAL (Figure 1), a system that addresses the above challenge by synthesizing declarative queries on behalf of users from a small number of labeled video segments. Put another way, EQUI-VOCAL Evolves Queries for Users Iteratively and is part of our larger VOCAL system [20]. In our example, a user provides as few as two positive and ten negative examples containing the event of interest (see Section 5). EQUI-VOCAL then synthesizes a declarative query and executes it on the remaining large pool of video data to identify other examples of the desired event. The source code of EQUI-VOCAL is available at [1].

EQUI-VOCAL supports users’ search for complex events without requiring any specific domain knowledge, with limited effort, and without requiring precise declarative specifications or sketches. Similar to other systems, we use the insight that while most user queries are new and unseen, they are usually composed of known, previously seen atoms. Computer vision models for common atoms

already exist such as objects (e.g., “car”, “backpack”) and their spatial and semantic relationships (e.g., “left of”, “holding”). Formally, such a composition of visual scenes is referred to as a scene graph in the computer vision community [36, 44] and was developed from its cognitive grounding in human perception [9, 47, 83]. Key to EQUI-VOCAL’s contribution is to encapsulate spatio-temporal scene graphs in its data model and use them to define a query language. A spatio-temporal scene graph conceptualizes the contents of a video as a sequence of graphs, each graph representing a single video frame. Each graph contains vertices, which represent objects in the frame; edges represent the relationships between those objects. Each object can possess a set of attributes that describe its properties (e.g., “red”, “leather”). EQUI-VOCAL extracts relevant data from each video using user-provided functions: i.e., pre-existing detectors and classifiers; it synthesizes queries as a composition of extracted scene graph atoms. We show that EQUI-VOCAL’s data model and query language, both based on the relational model, can express a variety of compositional queries.

Leveraging scene graphs, EQUI-VOCAL contributes a new query synthesis approach that finds user events with far fewer labeled examples than would be required to train a specialized machine learning model directly, and that works on noisy, video-scale data, and complex events. To support query synthesis in such environment, EQUI-VOCAL solves two technical challenges: it reduces **computational effort** and **user effort**.

EQUI-VOCAL reduces **computational effort** by limiting query search using scene graphs, by pruning search paths using beam search, and by avoiding expensive database operations. First, unlike prior query-by-example techniques that synthesize arbitrary SQL [23, 49, 59, 70, 73], EQUI-VOCAL reduces the search space by limiting the query search to sequences of scene graphs. Second, synthesizing queries over sequences of scene graphs can still be a computationally slow process to traverse the search space of possible queries. Existing query-by-example systems enumerate all possible queries; although pruning techniques like equivalence classes [71], over-approximation [73], and lifting projection operators [70] can be used to reduce the search space, these mechanisms are not sufficient to make exhaustive exploration tractable. Instead, EQUI-VOCAL adopts a beam search strategy to explore the query space efficiently. Beam search limits exploration to a subset of the most promising branches at each step. Third, executing the many candidate queries on the user examples is prohibitively expensive. Existing systems [70, 73] evaluate candidate queries with many joins and thus do not scale well when the size of user examples becomes large. EQUI-VOCAL carefully generates efficient queries that avoid expensive operations such as recursive joins. EQUI-VOCAL comes with a set of optimizations to generate efficient SQL statements and uses the PostgreSQL database engine to execute them.

EQUI-VOCAL reduces **user effort** by using active learning and by being robust to noise. With active learning, EQUI-VOCAL reduces the number of labeled examples needed: Instead of asking a user to provide all examples up front, EQUI-VOCAL iteratively requests labels of carefully selected additional examples to reduce the uncertainty in query synthesis. Noise can naturally creep into systems that interface with user labeling, machine learning models, and potentially ambiguous real-world events. Distinct from other existing systems [55, 70], EQUI-VOCAL searches for queries that



Figure 2: Example frames of multiple, simultaneous car-motorcycle interactions (generated using [29]). EQUI-VOCAL represents video content as a sequence of region graphs in its data model. Each region graph models a single video frame (left figure), with nodes representing objects and edges representing relationships. A region graph is a subset of the full scene graph (not shown).

best match potentially noisy data and input. It also retains imperfect query candidates at every iteration and uses regularization to prevent overfitting to noise or limited user input.

In summary, EQUI-VOCAL makes the following contributions:

- We introduce an expressive data model and a query language based on spatio-temporal scene graphs (Section 2).
- We propose a new approach that efficiently synthesizes the user’s intended query from examples. We limit the query search space using scene graphs, prune search paths using beam search, leverage active learning to reduce user effort, and handle noisy data (Section 3).
- We implement a set of optimizations to generate efficient SQL query statements and reduce computational effort during query synthesis (Section 4).
- We evaluate our approach on [synthetic and real datasets](#) [6, 81] and show that it outperforms two baselines [55, 70]—in terms of F1 score, synthesis time, and robustness to data noise—and can flexibly synthesize complex queries that the baselines do not support. [We also conduct a user study to show the performance of real users using EQUI-VOCAL.](#) (Section 5).

Overall, EQUI-VOCAL is an important step toward making video database management systems more accessible to experts and non-experts alike, by easing the task of expressing queries over videos.

2 EQUI-VOCAL DATA MODEL

This section describes EQUI-VOCAL’s data model and query language, which we briefly introduced in our vision paper [20], but develop in depth here. Section 3 shows how EQUI-VOCAL synthesizes queries from user input using this data model.

For ease of presentation, we use a simplified, running example, where a traffic engineer seeks to find instances of “a car arriving from the left and passing a motorcycle at the intersection.” Figure 2 shows two representative frames from a video that contains such an event. We show other example queries in Section 5.

2.1 Scene graphs as our data model

EQUI-VOCAL represents a video V as a set of short, non-overlapping *video segments*, $v \in V$ (5-second segments in our prototype implementation). Each video segment is a sequence of N

Table 1: Relational schema representation of data model.

Objects(vid, fid, oid, cid, x_1, y_1, x_2, y_2)
Relationships(vid, fid, rid, oid ₁ , pid, oid ₂)
Attributes(vid, fid, oid, key, value)

frames $\{f_1, \dots, f_N\}$. The visual content of each frame is represented by a scene graph [44]: A *scene graph* $g_i = (\mathbf{o}_i, \mathbf{r}_i)$ contains the set of all objects \mathbf{o}_i in a frame, along with a set of all relationships \mathbf{r}_i between those objects. Often a scene graph contains more information than is necessary to identify an event, and so the literature also defines a *region graph* g_{ij} , which is a subgraph of g_i , i.e., $g_{ij} \subseteq g_i$. Figure 2 (left) shows an example frame and region graph.

We define an *object* in a frame as $o = (vid, f_i, oid, cid, bbox)$, where f_i is the sequence number of frame i in video segment, vid , oid is a unique identifier of the object in the video segment, cid is the identifier for the class of the object (e.g., “car”, “motorcycle”), and $bbox$ is the bounding box containing the object in frame, f_i . A $bbox$ is represented by its upper-left and bottom-right coordinates, i.e., $bbox = (x_1, y_1, x_2, y_2)$.

Objects can have intra-frame *relationships* defined as $r = (vid, f_i, rid, oid_{sub}, pid, oid_{tar})$, where rid is a unique identifier of the relationship in frame, f_i . Subject, o_{sub} , is connected to target, o_{tar} , with the relationship class identifier, pid (e.g., “near” or “holds”). Both subject and target belong to frame f_i : i.e., $o_{sub}, o_{tar} \in \mathbf{o}_i$.

Objects can have *attributes* $a = (vid, f_i, oid, k, v)$, where k is the name of the attribute, v is the value of the attribute, vid, f_i and oid identify the video segment, frame, and object. EQUI-VOCAL distinguishes *state* and *property* attributes. The former change over time and are typically computed from the bounding box of an object (e.g., “location=bottom”). The latter capture intrinsic properties of objects and are immutable (e.g., “color=red”).

Finally, an *event* e is a temporally ordered sequence of region graphs $e = (eid, \{g_1, \dots, g_k\})$. Region graphs in an event do not need to be contiguous or distinct.

Example. Suppose that the two frames in Figure 2 are the 10th and 15th frames of a video segment V1, and that the motorcycle and car are the 7th and 9th objects detected in V1. Then, for the left frame, we generate the region graph $g_1 = (\mathbf{o}_1, \mathbf{r}_1)$, where: $\mathbf{o}_1 = \{o_{11}, o_{12}\}$ represents the car $o_{11} = (V1, F10, OID9, car, bbox_1)$ and the motorcycle $o_{12} = (V1, F10, OID7, motorcycle, bbox_2)$ and $\mathbf{r}_1 = \{r_{11}\}$ contains a relationship $r_{11} = (V1, F10, RID1, OID9, leftOf, OID7)$. The car also has an attribute $a_{11} = (V1, F10, OID9, location, bottom)$. We can define the region graph g_2 for the right frame similarly. The only difference will be the relationship between the object will indicate that the car is now rightOf the motorcycle. Finally, the event $e = (EID1, \{g_1, g_2\})$ represents a car arriving from the left and passing a motorcycle at the intersection.

The relational schema in Table 1 captures the above data model. The benefit of using a relational schema is that we can execute relational queries to specify region graphs and find events of interest, which is flexible and follows the well-understood semantics of the relational model. For each video (or collection of related videos), EQUI-VOCAL creates a *view* with this schema. In Section 4 we describe when and how relations in the view are materialized.

To populate each relation, EQUI-VOCAL uses available user-defined functions (Figure 1). User-defined functions can be provided by the user or be available publicly in the form of existing machine

learning models, such as object detectors. Various user-defined functions can be declared in EQUI-VOCAL: (i) an object detector [62] that takes a video frame as input and outputs the set of objects and their bounding boxes, (ii) an object tracking algorithm [78] that takes objects in consecutive frames as input and, for each pair of objects, determines if they are the same, and (iii) a set of pre-trained models (e.g., [13]) or rules that can take two objects in the same frame as input and determine their relationship (e.g., “near”, “behind”, “riding”, “holding”) or that can take one object as input and determine its attributes (e.g., “location=bottom”, “color=red”). In our experiments, EQUI-VOCAL uses a general-purpose object detector [32] to locate objects and intrinsic attributes of objects to generate trajectories across frames [81].

2.2 Scene graphs as our query language

EQUI-VOCAL could execute arbitrary relational queries on the view defined above. However, this would form an intractable search space, making query synthesis unusably slow for most real-world applications. Instead, we define a query language that is more restrictive, affording a smaller search space and therefore, faster synthesis. We constrain queries to (i) a temporally ordered sequence of region graphs, (ii) a set of predicates, (iii) a set of duration constraints, (iv) a window specification, and (v) to output video segment identifiers. Using Datalog and with some abuse of notation, a query in EQUI-VOCAL can be expressed as:

$$q(vid) :- g_1, \dots, g_k, \mathbf{p}, \mathbf{d}, w, \text{ where:}$$

- A temporally ordered sequence of region graphs g_1, \dots, g_k specifies that a matching event consists of g_1 , followed by g_2 , followed by g_3 , etc. Each g_i is specified with a set of atoms: Objects, Relationships, and Attributes joined on a shared vid and fid . Moreover, each g_i can persist for multiple frames and there can be other frames between g_i and g_{i+1} .
- A set of predicates \mathbf{p} can be applied to objects, relationships, and attributes. In our example, predicates would specify that the query is looking for “car” and “motorcycle” objects, that the car needs to be “left of” then “right of” the motorcycle, and that the car should be at the “bottom” of the frame.
- A set of duration constraints \mathbf{d} can be applied to region graphs and define the minimum number of contiguous frames that a region graph g_i should be valid before transitioning to the next region graph g_{i+1} .
- A window specification w is the maximum number of frames that can separate g_1 from g_k .

For example, following the above restricted template, the event in Section 2.1 can be expressed with the following Datalog rules:¹

```
g1(vid, fid, oid1, oid2) :-
  Objects(vid, fid, oid1, 'car', _, _, _, _),
  Objects(vid, fid, oid2, 'motorcycle', _, _, _, _),
  Relationships(vid, fid, _, oid1, 'leftOf', oid2),
  Attributes(vid, fid, oid1, 'location', 'bottom'), oid1 != oid2.
```

The above rule will find frames in video segments that contain a car and a motorcycle, such that the car is on the left of the motorcycle, and the car is at the bottom of the frame, where the intersection

¹In this and the following examples we use English words instead of integers for cid and pid values to make the examples more readable

Table 2: Comparison between compositional video analytics systems.

	SVQ++ [12]	Chen et al. [17]	Caesar [50]	STAR [15]	VidCEP [80]	CVQL [46]	Quivr [55]	Rekall [24]	Ours
Object detection	✓	✓	✓	✓	✓	✓	✓	✓	✓
Object tracking		✓	✓	✓	✓	✓	✓	✓	✓
Relationship	✓		✓	✓	✓	✓	✓	✓	✓
Attribute				✓	✓			✓	✓
Conjunction		✓	✓	✓	✓	✓	✓	✓	✓
Sequencing			✓	✓	✓	✓	✓	✓	✓
Iteration		✓				✓	✓	✓	✓
Window		✓			✓			✓	✓
Query by example							✓		✓

is located. Next, the event will likely consist of a sequence of such frames, which can be captured with the following recursive rules:

```

g1_star(vid, fid, fid, oid1, oid2) :- g1(vid, fid, oid1, oid2).
g1_star(vid, fid_start, fid_end, oid1, oid2) :-
  g1_star(vid, fid_start, fid, oid1, oid2),
  g1(vid, fid_end, oid1, oid2), fid_end = fid + 1.

```

We could use equivalent rules to define $g2$ and $g2_star$. Finally, the query that returns matching video segments takes the form:

```

q(vid) :- g1_star(vid, fid11, fid12, oid1, oid2),
  g2_star(vid, fid21, fid22, oid1, oid2),
  fid21 > fid12, fid22 - fid11 < 1800

```

The predicate $fid21 > fid12$ indicates that the second sequence of region graphs should follow the first one. The predicate allows for a gap between sequences, which may arise, for example, if something obstructs the vehicles from the camera’s view. Finally, $fid22 - fid11 < 1800$ puts a time constraint on the event (a 30-second time-window, assuming 60 frames per second).

To summarize, EQUI-VOCAL’s query language is a subset of Datalog with recursion, expressed on a specific schema. In Section 4, we explain how we avoid executing expensive recursive queries.

2.3 Expressiveness of our data model

We compare the expressiveness of EQUI-VOCAL’s data model against other compositional video analytics systems in Table 2. Among them, SVQ++ [12] only supports spatial relationships between two objects, Chen et al. [17] only supports temporal queries that count co-occurring objects. Caesar [50], STAR Retrieval [15], and VidCEP [80] lack the important feature of *iteration* that allows a region graph to persist for multiple frames and thus cannot support duration constraints. CVQL [46] does not track objects and all its predicates are defined at the object class level. Quivr [55] has similar expressiveness to us, but is limited to trajectory queries. Rekall [24] introduces a flexible Python library for video event specification, but requires that users manually write and refine queries.

Our data model currently does not support tertiary relationships between three objects, such as “a person hitting a ball with a bat”. The closest approximation we have is “a person holding a bat” and “a bat hitting a ball”. We also do not support disjunctions or negations. Several existing systems have support for these operators. For example, Chen et al. [17] supports arbitrary CNF queries, Caesar [50] supports disjunctions, and Rekall [24] can flexibly support all three operators. However, the focus of these systems lies in query execution, rather than in learning query specifications from examples, which is the primary focus of this paper.

Datalog and scene graphs serve as the foundation of our query language. By building on the relational model and Datalog, we ensure that our queries have precise and well-understood semantics. By focusing on queries that specify a desired sequence of region graphs, we constrain the search space for queries, which accelerates synthesis, we are able to optimize the execution of those queries (compared with trying to support arbitrary recursive Datalog queries), and we are still able to capture events that occur in videos, where objects interact with each other in space and time.

3 QUERY SYNTHESIS

With our data model and query language defined, we now formally present the query synthesis problem statement, then describe all the components of our proposed solution.

3.1 Query synthesis problem statement

Following the aforementioned data model, a user would like to execute a query q_u on video database D that returns a set of video segment identifiers, $V_{output} = q_u(D)$. Given the user’s intended query, q_u , each video segment v_i can be seen as having a ground-truth label $y_i \in \{0, 1\}$ indicating whether it matches q_u . Initially, both the ground-truth labels and q_u are unknown because the user is unable to specify q_u and can only label video segments as positive or negative instances. The goal of EQUI-VOCAL is to synthesize a target query, $q_t \in Q$, that is the best approximation of q_u in its search space. When executed over database D , q_t should yield the best measure performance (e.g., F1 score):

$$q_t = \arg \max_{q \in Q} \text{measure}(q(D), q_u(D))$$

EQUI-VOCAL can request a label from the user O : $\hat{y}_i = O(v_i)$. Since user labels may be noisy, it is possible that $\hat{y}_i \neq y_i$. Given that enumerative search is intractable, EQUI-VOCAL uses a heuristic approach to find an approximately-best query \hat{q}_t to the objective, while reducing both user effort and query synthesis time.

3.2 Query synthesis algorithm overview

Algorithm 1 provides an overview of EQUI-VOCAL’s synthesis algorithm. It traverses the space of possible queries to synthesize a final target query that matches the user’s intent. The algorithm takes as input the set of unlabeled video segments, U , and a small set of labeled segments, L . L is provided by the user and should include both positive and negative examples of the desired event. In our experiments, we require as few as two positive and ten negative examples. While providing two positive examples requires some work from the user, such a setting is common in query-by-example approaches [23, 55, 61]. We leave starting with zero examples for future work. The algorithm also takes as input a set of user-defined functions, P , comprised of indicator functions for object classes (e.g., “car”), relationships (e.g., “near”), and attribute key-value pairs (e.g., “color=red”). Algorithm 1 enumerates P when expanding its search space.

The algorithm returns a set of target queries, Q_t , which is the top- k synthesized queries ranked by a performance measure (F1 score in our prototype implementation) and is updated regularly through

Algorithm 1: Query synthesis algorithm that returns top- k synthesized queries matching user input.

Input : U - set of unlabeled video segments
 L - set of labeled video segments
 P - set of user-defined functions
 b, bw, s_q, s_v, k - hyperparameters

Output: Q_t - set of top- k target queries

```

1  $S \leftarrow \{q_\emptyset\}$ 
2 while  $|S| > 0$  do
3    $S' \leftarrow \{\}$ 
4   foreach  $q \in S$  do
5      $S' \leftarrow S' \cup \text{EXPANDQUERY}(q, P)$ 
6   if  $|L| < b$  then
7      $L, U \leftarrow \text{PICKNEXTSEGMENTS}(L, U, S')$ 
8    $S \leftarrow \text{SAMPLEQUERIES}(S', L, bw)$ 
9    $Q_t \leftarrow Q_t \cup S'$ 
10   $Q_t \leftarrow \text{RETAINTOPQUERIES}(Q_t, L, k)$ 
11 return  $Q_t$ 

```

the search process. The learned queries can be applied to unseen videos to find video segments containing the matching event. By default, EQUI-VOCAL returns the top- k queries but then executes the best one over unseen videos. The user can also randomly sample one query from Q_t , execute multiple queries from Q_t and aggregate the results, or manually examine Q_t to pick the intended query. **If the user is not satisfied with the synthesized query, they can edit it directly.** The user can also restart the search with a larger number of initial examples by reusing the video segments labeled during the last session. Moreover, the user could provide a starter query to EQUI-VOCAL (e.g., a simple query or an earlier query) rather than starting from an empty query.

To populate Q_t efficiently, EQUI-VOCAL synthesizes queries in a bottom-up fashion. It starts with an empty query, q_\emptyset , and incrementally adds predicates to it, up to a certain complexity (EXPANDQUERY method on line 5 and Section 3.3). At each step, different predicates can be added to a query, expanding the search in multiple directions. To limit the size of the search space and ensure fast query synthesis, EQUI-VOCAL adopts a beam search-style strategy (SAMPLEQUERIES method on line 8 and Section 3.4).

An important challenge for EQUI-VOCAL is that learning a query from a small number of user-provided examples is difficult. To address this challenge, EQUI-VOCAL uses active learning to effectively guide the query synthesis process and identify good target queries with limited initial and additional user effort. Specifically, method PICKNEXTSEGMENTS on line 7 and in Section 3.5 uses active learning to select additional video segments for the user to label in order to effectively differentiate between multiple candidate subqueries, and expand the search in the most promising directions.

At the end of each iteration, method RETAINTOPQUERIES (line 10 and Section 3.6) maintains a list of top- k queries seen so far, which is larger than the number of queries selected for additional expansion, in case a query seen earlier in the search ends up with the best score on the final labeled set of segments, or, as mentioned above, to give users options if they would like to try alternative, high-performing queries.

The algorithm has several hyperparameters, including a labeling budget b (i.e., the maximum number of labels the user is willing to provide), the number of candidate queries to retain during exploration bw (i.e., the beam width), **the number of candidate queries, s_q , and the number of candidate video segments, s_v , sampled during active learning**, and the number of queries in the final answer k . Figure 3 illustrates the algorithm using the running example.

3.3 Query expansion

Existing query-by-example systems use sketch-based query synthesis approaches [55, 70, 73] to enumerate candidate queries. A sketch query is a query with unspecified parts in the form of holes and these approaches enumerate the search space by first generating high-level sketch queries and then filling them with low-level details. However, enumerative search is slow and memory-intensive. Inspired by execution-guided synthesis approaches [14, 35], which treat a program as a sequence of manipulations and use the results of partial programs to guide the search, EQUI-VOCAL explores the search space based on the results of executing intermediate queries on the examples. Instead of synthesizing sketch queries with uninstantiated holes that cannot be executed directly, or directly applying techniques from [14, 35], which require a large amount of data to train a neural synthesizer, EQUI-VOCAL expands queries by adding instantiated and executable constraints, executing partial queries to assess the promise of each explored path, and iteratively refining a query towards the target query.

In our synthesis algorithm, method EXPANDQUERY(q, P) takes as input a query q to expand, and a set of user-defined functions, P to construct more complex queries. The function returns a set of expanded queries as illustrated in Figure 3(a).

Our query synthesis approach uses a compact query notation, which can be seen as a DSL. The DSL captures the logical structure of the queries to synthesize and key query parameters, but omits the details of the full, underlying SQL (or Datalog). This approach is important for several reasons: First, since we do not generate arbitrary SQL, but rather queries that conform to the structure presented in Section 2.2, the DSL captures that structure precisely, simplifying the search space and guiding synthesis toward the correctly-structured queries. Second, this approach helps to decouple the logical query specification from the details of the SQL queries that are ultimately executed. As we present in Section 4, critical optimizations are necessary during the translation from our DSL to SQL to achieve efficient query execution.

In our DSL, we use a *variable* o to represent an object in a query. Different variables represent objects with different *oid*'s. All predicates of a region graph are connected by commas and are represented with shorthand notations that specify only their key-value pairs (for property attributes, e.g., `Color(o_1 , 'cyan')`), value (for state attributes, e.g., `Bottom(o_1)`), or class (for objects and relationships, e.g., `Car(o_1)`). Then, region graphs are connected in sequence with semicolons. For example, the query for the event from Section 2.1 can be represented as:

$$q = (\text{Car}(o_1), \text{Motorcycle}(o_2), \text{LeftOf}(o_1, o_2), \text{Bottom}(o_1)); \\ (\text{Car}(o_1), \text{Motorcycle}(o_2), \text{RightOf}(o_1, o_2), \text{Bottom}(o_1)))$$

We further use the notation $\text{Duration}(g, d)$ to require that the region graph g exist in *at least* d consecutive frames.

$P = \{\text{Car, Motorcycle, LeftOf, RightOf, Bottom}\}$, $bw = 2, k = 1$

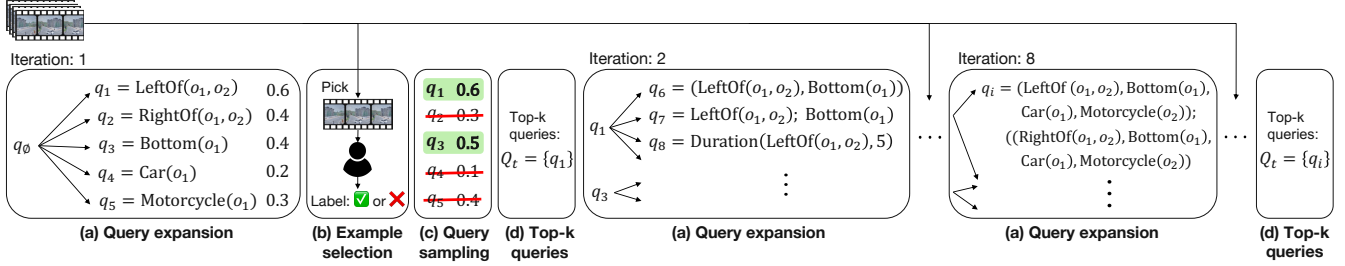


Figure 3: Running example of the query synthesis algorithm. The algorithm starts with q_0 and synthesizes queries by iteratively (a) expanding queries, (b) selecting new video segments for the user to label, (c) sampling a small set of queries for further expansion, and (d) updating a list of top- k queries after each iteration. The algorithm returns $Q_t = \{q_i\}$.

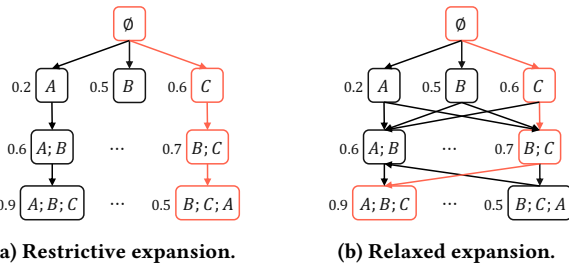


Figure 4: A restrictive rule constrains each query to have one construction path, while a relaxed rule allows for multiple paths. Though a relaxed rule results in a larger search space, it is more likely to find queries with high performance than a restrictive rule.

During query synthesis, EQUI-VOCAL expands queries written in our DSL. EXPANDQUERY takes any of the following three actions: (i) Graph construction (GC): Add a predicate to an existing region graph. (ii) Sequence construction (SC): Insert a new region graph consisting of one predicate into any position of the existing sequence of region graphs. (iii) Duration refinement (DR): Increment the duration constraint of an existing region graph in the sequence.

As shown in Figure 3(a), EQUI-VOCAL starts with an empty query $q_0 = q_0$. In iteration 1, EQUI-VOCAL takes action SC to expand q_0 . This results in q_1 to q_5 , each consisting of a single region graph with one predicate drawn from P . In iteration 2 of Figure 3(a), EQUI-VOCAL first expands $q_1 = \text{LeftOf}(o_1, o_2)$. Performing action GC leads to $q_6 = (\text{LeftOf}(o_1, o_2), \text{Bottom}(o_1))$; SC leads to $q_7 = \text{LeftOf}(o_1, o_2); \text{Bottom}(o_1)$; and DR leads to $q_8 = \text{Duration}(\text{LeftOf}(o_1, o_2), 5)$, assuming the granularity of Duration is 5 frames.

Deciding which actions to take to expand queries is an important design decision in EQUI-VOCAL. Imagine the search space as a directed acyclic graph (DAG), where each node represents a possible query in the search space, the root node represents the empty query q_0 , and the query of each child node is constructed by applying one action to its parent node. We consider two extreme expansion rules: A restrictive rule (Figure 4a) only allows each query to have one construction path in the DAG, while a relaxed rule allows each query to be generated through all possible permutations of actions with multiple construction paths (Figure 4b). Our early experiments showed that the restrictive rule led to poor performance: In some

cases, queries with high performance were not found because their ancestor queries (i.e., intermediate parent queries) were not good and were getting pruned. Since different predicates and their combinations have different selectivity and contribute differently to the final query performance, the relaxed rule allows the algorithm to focus on synthesizing the more dominant part of the query during early iterations, avoiding all paths to the target query being accidentally pruned. The cost of a relaxed rule is a larger search space and slower query synthesis. In the example of Figure 4, queries are constructed following the paths highlighted in blue, assuming only the best query is expanded at each step. The restrictive rule selects the query $B; C; A$ with a score of 0.5 rather than $A; B; C$ with a score of 0.9, because A has a lower F1 score than C and B . On the other hand, using the relaxed rule selects $A; B; C$ by first constructing C , then adding B and A to the sequence. EQUI-VOCAL follows the relaxed rule: GC can add any predicates that are not already in the region graph (predicates of the same user-defined function but different variables are considered different); SC can insert a new region graph before and after any existing region graph; DR can increment the duration constraint of any existing region graph.

3.4 Beam search

When traversing the search space, we can **greedily expand only the top query or exhaustively expand all**. The former is quick to compute but may not find the target query at the end, while the latter is optimal but comes with a prohibitive computational cost. EQUI-VOCAL uses beam search to balance query performance and synthesis efficiency. **Beam search has a wide range of applications in problems with large search spaces, especially in NLP [45, 51, 72]. The greedy approach can be viewed as a special case of the beam search with a beam width of one, and the exhaustive search is equivalent to a beam search with an infinitely large beam width.** Beam search reduces runtime by limiting the number of explored branches at each iteration. However, the search outputs are not guaranteed to be optimal. Search quality depends on how branches are expanded, scored, and pruned. In our approach, method SAMPLEQUERIES(S', L, bw) retains the top bw queries to expand by evaluating the F1 score of the S' candidate queries on the set of labeled video segments L (see Figure 3(c)). **Prior work has analyzed the theoretical properties of beam search under certain assumptions (e.g., monotonicity of**

scoring functions [54], Bayes optimality of tree models under approximations [84]). While in this paper, we directly use the F1 score as the scoring function and to retain top queries, other more sophisticated scoring functions and pruning techniques can be used as alternatives [2, 54, 72]. We show the effectiveness of our synthesis algorithm empirically in Section 5.

3.5 Active learning

One challenge with asking the user for only a handful of examples of the intended event is that we risk overfitting, but asking the user to find a larger number of initial examples is difficult. To address this challenge, we use active learning during query synthesis.

Many active learning methods have been proposed in the literature with the goal of labeling samples that maximally improve a model trained on those samples. E.g., uncertainty-based sampling [48], estimated error reduction [64], and core-set approach [66]. In our work, we use active learning to label samples that help us identify which candidate queries are better than others. To do so, we need to label samples where candidates disagree: Therefore, we use disagreement-based active learning [43]. At every iteration, EQUI-VOCAL asks the user for a handful of additional labels to differentiate between the bw queries retained from the previous iteration. Intuitively, this method picks the video segments where the retained queries disagree the most. A similar idea appears in the query-by-committee algorithm [68] and has been used in other program synthesis and query synthesis systems [37, 55]. EQUI-VOCAL’s contribution is to incorporate active learning in each iteration of the search process, ensuring an interaction-level labeling experience. Using active learning reduces the number of data points a user has to provide; additionally, we posit that it is easier for users to label system-selected examples than to come up with their own.

During each call to `PICKNEXTSEGMENTS(L, U, S')`, EQUI-VOCAL computes a score for a sample of unlabeled video segments U over the candidate queries S' and then picks the video segments with the largest disagreement. The score of each sampled, unlabeled video segment is computed as the weighted disagreement between the candidate queries. The weight of each candidate query is set to its regularized performance over the labeled set L (Section 3.7). While the algorithm in [43] is designed for the setting where labeling candidates are streamed, EQUI-VOCAL instead maintains a pool of candidates. Therefore, for each call to `PICKNEXTSEGMENTS`, EQUI-VOCAL computes the score for a sample of unlabeled video segments s_v over a sample of candidate queries s_q and then picks the best one. The function updates L and U given the new user labels. As shown in Figure 3(a), EQUI-VOCAL generates five candidate queries q_1 to q_5 in iteration 1. Among them, q_1 has the highest score 0.6, while q_2 and q_3 give the same second highest score 0.4. EQUI-VOCAL requests a new video segment to be labeled (Figure 3(b)), which distinguishes q_3 from q_2 (Figure 3(c)).

Before query synthesis begins, users can set the labeling budget as a hyperparameter. EQUI-VOCAL precomputes the number of iterations of query expansion it will perform and uniformly divides the labeling budget among iterations. At every iteration, EQUI-VOCAL asks for new labels only if it has a labeling budget left to do so; otherwise, it proceeds to synthesize queries without requesting

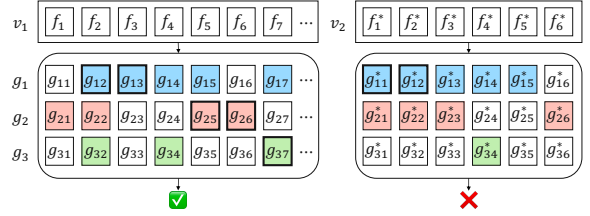


Figure 5: Query execution example. EQUI-VOCAL reduces intermediate result sizes by computing the *earliest* matching sequences for each region graph specification.

new labels. EQUI-VOCAL precomputes the number of iterations by relying on the hyperparameters (Section 4) that bound the search process and the query expansion rules (Section 3.3), which increments the complexity of synthesized queries in each iteration.

3.6 Retaining top queries

At the end of each iteration, EQUI-VOCAL updates its list of candidate final queries in order to retain k best performing ones, as measured by their F1 scores on the labeled dataset. `RETAINTOPQUERIES(Q_t, L, k)` evaluates all candidate queries Q_t on labeled set L and returns the top k (Figure 3(d)).

In Figure 3(d), at the end of iteration 1, EQUI-VOCAL stores q_1 in Q_t because $k=1$, and q_1 has the highest score. When the algorithm terminates, EQUI-VOCAL returns q_1 as the final query. In our evaluation, we set the default value of k to 100 (and to 1000 for a more complex dataset), which ensures both low overhead and high-performing final queries.

3.7 Regularization

EQUI-VOCAL retains top queries using their F1 scores on the smaller L labeled set. This can lead to overfitting since there are likely too few training examples to accurately evaluate each candidate query. To prevent overfitting, we regularize the score of each candidate query by adding the term: $score_{reg}(q) = score(q) - \lambda \cdot R(q)$, where λ controls the importance of the regularization term. $R(q)$ represents the complexity of the query q : $R(q) = \sum_{i=1}^k (\alpha_1 n_{pi} + \alpha_2 n_{di} + \alpha_3 n_{di} n_{pi})$. Here, k is the number of region graphs in q , n_{pi} is the number of predicates in the i th region graph g_i , and n_{di} denotes the scale of the duration constraint of g_i . α_1 , α_2 , and α_3 are hyperparameters that control the importance of each term.

4 QUERY EXECUTION

As discussed in Section 3.3, we convert queries in our DSL into SQL and use a relational engine (PostgreSQL in our prototype) to execute them. In this section, we discuss important optimizations that we apply during this translation process.

Query translation algorithm. In Section 2.2, we show that queries over videos are naturally recursive. Such queries, however, are slow to execute. To avoid recursion, we leverage the observation that those queries express the idea of iteratively matching a region graph in a *contiguous sequence* of frames, rather than arbitrary recursion. Therefore, we can express them using window functions instead of recursion.

As a second optimization, we note that a query q in our DSL (Section 3.3) takes as input a set of video segments V and returns

```

CREATE VIEW g1_windowed AS (
SELECT vid, fid,
oid1, oid2,
lead(fid, d1 - 1, 0) OVER (
PARTITION BY vid, oid1,
oid2 ORDER BY fid
) as fid_offset
FROM g1
);

CREATE VIEW g1_iterated AS (
SELECT vid,
min(fid_offset) AS fid,
oid1, oid2
FROM g1_windowed
WHERE fid_offset
= fid + (d1 - 1)
GROUP BY vid, oid1, oid2
);

CREATE VIEW g2_filtered AS (
SELECT t1.vid, t2.fid,
t1.oid1, t1.oid2
FROM g1_iterated t1, g2 t2
WHERE t1.vid = t2.vid
AND t1.oid1 = t2.oid1
AND t1.oid2 = t2.oid2
AND t1.fid < t2.fid
);

```

(a) Q1: window (b) Q2: iterate (c) Q3: filter

Figure 6: SQL snippets. EQUI-VOCAL generates efficient SQL queries by avoiding recursions and pruning intermediate results.

all segments in V containing at least one event that matches q . Therefore, instead of finding all satisfying events for each video segment, the query execution needs to find only one. We leverage this observation to reduce intermediate result sizes by producing SQL that efficiently computes the *earliest* matching sequences for each region graph specification. This optimization applies to queries without window specifications and whose duration constraints are of the form “>” or “>=”, which are the only types of queries that EQUI-VOCAL currently generates.

As a concrete example, consider Figure 5. Assume we want to execute a query $q = \text{Duration}(g_1, 2); \text{Duration}(g_2, 2); g_3$, where $g_1 = \text{Far}(o_1, o_2)$, $g_2 = \text{Near}(o_1, o_2)$ and $g_3 = \text{Behind}(o_1, o_2)$. Also, we only consider one permutation of objects for each video segment in this example for simplicity. The event that q looks for consists of a contiguous sequence of g_1 for at least $d_1 = 2$ frames, followed by a contiguous sequence of g_2 for at least $d_2 = 2$ frames, etc.

Consider video segment v_1 . For the first region graph g_1 , we only need to extract the earliest matching segment of g_1 , which is $e_{11} = \{g_{12}, g_{13}\}$. This is because, for every satisfying event for the query, we can replace its matching segment of g_1 with the earliest one and the resulting event will still be a match to the query. $e_2 = \{g_{13}, g_{14}, g_{25}, g_{26}, g_{37}\}$ is a matching event for q . By replacing $e_{12} = \{g_{13}, g_{14}\}$ with $e_{11} = \{g_{12}, g_{13}\}$, we get $e_1 = \{g_{12}, g_{13}, g_{25}, g_{26}, g_{37}\}$, which is still a matching event for q . For subsequent region graph g_2 , we first use the earliest matching segment from g_1 to retain matching frames of g_2 that are temporally after the end frame of the segment, which are g_{25} and g_{26} . Then, we can use the same method as before to find the earliest matching segment from g_2 , which is $e_{21} = \{g_{25}, g_{26}\}$. The same procedure can be applied to g_3 , giving us $e_{31} = \{g_{37}\}$. Thus, the earliest matching event for q in v_1 is e_1 . Video segment v_2 does not contain any matching event of q .

The above algorithm can be expressed using SQL queries, as shown in Figure 6. Q1 partitions the data on video ID and each unique permutation of groups of objects so that each group of objects is analyzed separately, and sorts the data on frame ID. Next, for each row, it gets the current frame ID as well as the frame ID that is d_1 frames after the current frame ID, or 0 if no such frame exists. The result of Q1 gives a table of intervals. Q2 then finds the earliest matching segment for each combination of video and groups of objects. Together, Q1 and Q2 find the earliest matching segment for $\text{Duration}(g_1, 2)$ without using recursive joins. Q3 uses the earliest matching segment from g_1 to determine where to look for matching segments in g_2 . The example SQL snippets only contain two objects $oid1$ and $oid2$. In general, Q1 and Q2 partition and group the data by all objects in the region graph g_i , and Q3 specifies all the

constraints on objects across two region graphs in the where clause. We demonstrate the impact of both optimizations in Section 5.5.

Caching. We implement an application-level cache to reuse sub-query results. EQUI-VOCAL generates SQL queries as described above to find matching region graphs in the sequence specified by the DSL query one by one. We cache the intermediate results of all prefixes on the set of video segments to allow other queries sharing the same sub-queries to reuse the results. For example, when executing the query $q = g_1; g_2; g_3$ on video segments v_1 and v_2 , we cache the results of $q_1 = g_1$, $q_2 = g_1; g_2$, and $q_3 = g_1; g_2; g_3$ on v_1 and v_2 . Later on, if a query $q' = g_1; g_2; g_4$ is executed on v_1 and v_3 , EQUI-VOCAL will reuse the cached results of $q_2 = g_1; g_2$ on v_1 to improve performance.

Bounding the search space. EQUI-VOCAL synthesizes queries up to a certain maximum size to ensure that the synthesis algorithm eventually terminates. Assume the number of user-defined functions for object classes and attributes is m_1 and the number of user-defined functions for relationships is m_2 . We bound the query search space using a set of hyperparameters: the maximum number of region graphs (n_g) in a query, the maximum number of predicates (n_p) in the query, the number of possible values a duration constraint can take (n_d), and the number of unique objects allowed in a query (n_v). The size of the search space is then $|Q| = O((n_g(n_v m_1 + n_d^2 m_2))^{n_p} \cdot n_d^{n_g})$.

Predicate evaluation. The current implementation of EQUI-VOCAL populates the Objects relation and the property attributes in the Attributes relation before query synthesis (see Table 1), by executing ML models on all video frames. The Relationships relation and the state attributes in the Attributes relation are computed lazily during query execution since they do not require ML models in our prototype, and are thus inexpensive to compute. In general, optimizing what information is computed before query synthesis and what is computed lazily is not the focus of this paper.

To simplify SQL query generation, we implement all predicates (except for join predicates) in EQUI-VOCAL as user-defined functions that take attributes and bounding box coordinates as input and return boolean values. In our prototype, we use PostgreSQL and implement user-defined functions for state and relationship predicates that operate on bounding boxes, and for property predicates that operate on key-value pairs.

While EQUI-VOCAL provides the above user-defined functions, the user can also provide additional user-defined functions incrementally as they use the system, and they can be shared and reused across queries and users [76]. In practice, EQUI-VOCAL has to limit the number of user-defined functions to a reasonable amount to ensure the efficiency of query synthesis.

5 EVALUATION

We conduct an experimental evaluation of EQUI-VOCAL. First, we show that **on both synthetic and real-world datasets**, compared to existing systems, EQUI-VOCAL reduces the query synthesis time by 1-2 orders of magnitude, achieves comparable or better F1 scores under the same labeling budget, is more robust to noisy data, and explores and executes queries more efficiently. Second, we show that EQUI-VOCAL is capable of synthesizing more complex, flexible queries over arbitrary scene graphs, which existing systems

Table 3: Example queries written for the trajectories dataset. “Pos %” is the percentage of positive examples in the dataset.

ID	Query	Description	Pos %
TQ1	(Near(o_1, o_2), Bottom(o_1))	o_1 is close to o_2 while o_1 is at the bottom.	7.0%
TQ2	Far(o_1, o_2); Near(o_1, o_2); Far(o_1, o_2)	Two objects move from far to close, then to far again.	7.5%
TQ3	Far(o_1, o_2); (Near(o_1, o_2), Behind(o_1, o_2))	o_1 and o_2 are far away, then they move close and o_1 is behind o_2 .	12%
TQ4	Far(o_1, o_2); (Near(o_1, o_2), Behind(o_1, o_2), Left(o_1))	o_1 and o_2 are far apart, then they move close and o_1 is behind o_2 and o_1 is on the left.	6.5%
TQ5	(FrontOf(o_1, o_2), Top(o_1))	o_1 is in front of o_2 while o_1 is at the top.	45%
TQ6	Near(o_1, o_2); Far(o_1, o_2)	Two objects move from close to far apart.	10%
TQ7	(Near(o_1, o_2), Left(o_1), Behind(o_1, o_2))	o_1 is close to and behind o_2 while o_1 is on the left.	8.5%
TQ8	(Far(o_1, o_2), Bottom(o_1)); Near(o_1, o_2)	o_1 at the bottom is far from o_2 , then they move close.	6.9%
TQ9	(Far(o_1, o_2), Left(o_1)); (Near(o_1, o_2), Left(o_1))	o_1 and o_2 move from far to close while o_1 is on the left.	10%
TQ1D	Duration(Far(o_1, o_2), 5); Near(o_1, o_2); Far(o_1, o_2)	Two objects are far apart for at least 5 frames, then they move close, then they are far again.	5.6%
TQ2D	Duration(LeftOf(o_1, o_2), 5); (Near(o_1, o_2), Top(o_1));	o_1 is on the left of o_2 for at least 5 frames, then they move close to each other and o_1 is at the top, then o_1 is on the right of o_2 for at least 5 frames.	6%
TQ3D	Duration((Frontof(o_1, o_2), Left(o_1)), 15);	o_1 is in front of o_2 while o_1 is on the left for at least 15 frames, then o_1 moves to the right of	8.3%
	Duration((Left(o_1), RightOf(o_1, o_2), Top(o_1)), 5)	o_2 while o_1 is at the top left for at least 5 frames.	

Table 4: Query configurations for the scene graphs dataset.

Query	relationship & state	property	region graph	duration
Easy	3	1	1	No
Medium	5	2	3	No
Hard	5	2	3	Yes

cannot handle. **Third, We conduct a user study to demonstrate the effectiveness and usability of EQUI-VOCAL. We further compare EQUI-VOCAL with a machine learning method and conduct an ablation study by varying the various design choices outlined in the previous sections.**

Baselines. To the best of our knowledge, there are no existing systems that can synthesize queries over scene graphs. The most similar system to EQUI-VOCAL is Quivr [55], which synthesizes queries over trajectories. Since object trajectories can be represented using scene graphs, we compare our system against Quivr. We also compare against PATSQL [70], which is a state-of-the-art query-by-example system for relational data.

Predicates. For the synthetic dataset, we use 13 predicates in experiments: six relationship predicates (Near, Far, LeftOf, RightOf, FrontOf, and Behind), four state predicates (Left, Right, Top, Bottom), and three property predicates (Color, Material, and Shape). We consider eight colors, two materials, and three shapes. Property predicates are only used for the scene graphs dataset. For duration constraints, we consider three possible values: $\text{duration}(g) \geq 5, 10, \text{ or } 15$ frames. Section 4 discussed how EQUI-VOCAL evaluates these predicates. For the real dataset, we use nine predicates: two relationship predicates (Faster, Near) and eight state predicates (LaneK, Stopped, HighAccel). LaneK detects whether a car is in lane K, and we identify five lanes in the video.

Data. We evaluate our system on both synthetic and real-world datasets. We first evaluate on the CLEVRER dataset [81], which comprises synthetic videos of moving objects. This dataset includes a variety of geometric shapes interacting in space and time, and comes with ground truth data, facilitating testing queries with varying complexities. We create two benchmarks from this data: trajectories and scene graphs datasets.

Trajectories dataset. We create a first dataset to test queries over trajectories, which baseline systems support. We extract 10,080 pairs of object trajectories that overlap in time from 500, 5-second video segments. Each trajectory pair is essentially a temporally ordered sequence of bounding box pairs $b = (x_{a1}, y_{a1}, x_{a2}, y_{a2}, x_{b1}, y_{b1}, x_{b2}, y_{b2})$ representing two objects in a

video segment. We manually generate a set of queries with varying complexities (Table 3). To generate ground truth labels, we run each target query on the dataset. We sample 500 trajectory pairs as training data (i.e., data used during query synthesis) and use the rest as test data (i.e., to measure the quality of synthesized queries). **Scene graphs dataset.** This more complex dataset contains scene graphs extracted from the CLEVRER dataset, which baseline systems do not support. We extract scene graphs from 10,000, 5-second video segments. For every frame of a video segment, we store the object track ID (*oid*), bounding box coordinates, and object attributes (shape, color, and material) of every object in the frame (the Objects and Attributes relations in Table 1). We sample 500 video segments as training data and use the rest as test data. We automatically generate three classes of queries with different complexities: *easy*, *medium*, and *hard*. Each generated query contains exactly three variables (i.e., three distinct objects), with configurations shown in Table 4. Each class contains 40 queries.

Real-world dataset. We test on a 50-minute traffic video from the YTStreams dataset [6]. The dataset comes with car trajectories, and we further extract the velocity and acceleration of each car trajectory as the object attributes, following the same procedure described in [55]. From the video, We create 72,159 pairs of overlapping car trajectories, using half of them as training data and the rest as test data. As shown in table 5, we adopt 13 queries from [55] for our evaluation, with some adjustments, including the use of a different in-lane detection method, removal of real-valued parameters from predicates, and expression of queries using scene graphs, and the introduction of additional queries with two scene graphs. These queries capture a wide range of car behaviors.

Metrics. We report the F1 score and query synthesis time. We synthesize queries using the training set and report the F1 score of the query (or the median F1 score if there are multiple queries with the same best score on the training set) over the test set. Each experiment is run 20 times for the trajectories and real-world datasets and five times for the scene graphs dataset, and we report the median F1 score and query synthesis time over these runs.

Implementation details. We implement our prototype in Python with PostgreSQL as the backend. We conduct all experiments except for the user study on a computing cluster with Intel Xeon Gold 6230R CPUs at 2.10GHz. When measuring runtimes, we request one node with one core and 100GB of RAM. Unless otherwise specified, we configure EQUI-VOCAL as follows. For the trajectories

Table 5: Example queries written for the real-world dataset. “# Pos ” is the number of positive examples in the dataset.

ID	Query	Description	# Pos
WQ1,2,3	(LaneA(o_1), LaneA(o_2), Near(o_1, o_2))	o_1 and o_2 are close and in the same lane.	164, 140, 228
WQ4,5,6	(LaneA(o_1), HighAccel(o_1)); (LaneA(o_2), HighAccel(o_2))	In lane 1, o_1 accelerates rapidly and then o_2 accelerates rapidly.	790, 495, 657
WQ7	(LaneA(o_1), LaneB(o_2)); (LaneB(o_1), LaneB(o_2))	o_1 is turning from lane A into lane B while o_2 is in lane B.	105
WQ8,9	(LaneA(o_1), LaneC(o_2)); (LaneB(o_1), LaneC(o_2))	o_1 merges from lane A into lane B while o_2 is in lane C (which is next to lane B).	492, 216
WQ1,2D	Duration((LaneA(o_1), LaneB(o_2), Near(o_1, o_2)), 5)	o_1 and o_2 are in adjacent lanes and close for at least 5 frames.	177, 435
WQ3,4D	Duration((LaneA(o_1), LaneB(o_2), Faster(o_1, o_2)), 5)	o_1 and o_2 are in adjacent lanes and o_1 is faster than o_2 for at least 5 frames.	471, 148

Table 6: Query synthesis time (median, in seconds) for each method to achieve at least 0.9 F1 scores. EQUI-VOCAL successfully learns all queries with at least 0.9 F1 scores and is faster than (or at least comparable to) the two baselines. (NA: not applicable, —: failed due to insufficient F1 score or timeout)

Method	Simplified									Normal											
	TQ1	TQ2	TQ3	TQ4	TQ5	TQ6	TQ7	TQ8	TQ9	TQ1	TQ2	TQ3	TQ4	TQ5	TQ6	TQ7	TQ8	TQ9	TQ1D	TQ2D	TQ3D
PATSQL	1.54	—	538	—	4.00	1.93	552	—	—	NA	NA	NA	NA	NA	NA	NA	NA	NA	NA	NA	NA
Quivr	10.5	5.77	27.9	94.2	13.5	4.36	47.7	16.7	—	7228	7428	8185	—	7839	3683	—	8756	—	—	—	—
Ours	3.57	1.85	17.1	46.6	4.36	1.66	18.5	22.7	20.6	75.6	125	106	185	50.4	61.1	106	110	107	223	166	183

dataset and the real-world dataset, we search for queries with up to 5 predicates across up to 3 region graphs. We use beam width $bw = 10$, $\lambda = 0.01$ for regularization (with $\alpha_1 = \alpha_2 = 1$, and $\alpha_3 = 0.1$, see Section 3.7), and we set $k = 100$, $s_q=100$, and $s_v = 100$. For the scene graphs dataset, we search for queries with up to 7 predicates, 3 region graphs, and 3 objects. Since the dataset is more complex and challenging, we use a smaller λ (because the query complexity term, $R(q)$ has a greater absolute value) and a greater k . We use beam width $bw = 10$, $\lambda = 0.001$ for regularization (with $\alpha_1 = \alpha_2 = 1$, and $\alpha_3 = 0.1$), and we set $k = 1000$, $s_q=100$, and $s_v = 100$.

The user study is conducted on an AWS EC2 c6id.4xlarge instance with 16 vCPUs and 32GB of RAM. We search for queries with up to 7 predicates, 3 region graphs, and 3 objects. For duration constraints, we consider three possible values, 25, 50, and 75 frames, which translate to 1, 2, and 3 seconds. To improve the interactivity of the system, we use a smaller beam width $bw = 5$ and a smaller sample of candidate queries $s_q = 25$ for active learning. We set $s_v = 100$, $\lambda = 0.001$ and $k = 100$.

We consider two variants of Quivr. As per the original paper, we limit the number of atomic predicates in Quivr’s queries to 5 and the depth of the nested constructs to 3, which leads to a similar search space as EQUI-VOCAL. When considering queries without duration constraints (e.g., TQ1-TQ9), we omit Kleene star operators from its search space. Otherwise (e.g., TQ1D-TQ3D), we include Kleene star in the query expansion and add one more predicate MinLength_θ , which checks whether the duration of the input is at least θ frames. Quivr returns all queries that match the examples, so we select the queries with the simplest structure (which is determined by the number of atomic predicates, and, if the former is the same, by the depth) and report their median F1 score.

Because PATSQL requires that *all* user-provided input tables be used in the solution query, when comparing against PATSQL, we restrict all systems to only the candidate predicates that appear in the target query. Because PATSQL cannot handle large tables efficiently, we also downsample each trajectory by 75% (we keep one frame out of four) to reduce the size of the input tables. We refer to this configuration as *simplified tasks*.

5.1 Results against baselines on trajectories

We evaluate EQUI-VOCAL against the two baselines on the trajectories dataset and the set of queries in Table 3. For TQ1-TQ9, we omit duration constraints from the search space. We run each method as follows. For each target query, we randomly select 2 positive and 10 negative examples from the training set and use them as the input to the method. Each method then asks for b additional examples during the search. For PATSQL, since it is not interactive, we simply sample b more examples randomly from the remaining dataset and provide the $12 + b$ examples to the system at the beginning. For Quivr and EQUI-VOCAL, we input the 12 initial examples, and each system actively requests more examples during the search process.

EQUI-VOCAL is faster than baselines and can find high-performance queries even for complex queries. Table 6 shows the query synthesis time of each query to achieve at least a 0.9 F1 score. For simplified tasks, EQUI-VOCAL outperforms baselines on 6 queries. PATSQL performs the best or close to the best when queries are simple (TQ1, 5, and 6) because these queries include only two predicates and PATSQL terminates once it finds one solution query. Quivr is slower than EQUI-VOCAL but comparable to it except for TQ9, in which case Quivr fails due to an insufficient F1 score of the synthesized queries. Under the normal setting, EQUI-VOCAL is significantly more efficient than Quivr and can find high-performance queries in hundreds of seconds even for complex queries with duration constraints, while Quivr cannot synthesize TQ4, TQ7, TQ9, and TQ1D-TQ3D within 4 hours due to the large number of queries that need to be explored in the enumerative search.

On simplified tasks, EQUI-VOCAL and QUIVR find queries with similar F1 scores and outperform PATSQL for the same labeling budget. Figure 7 shows the F1 score of each system when varying the user labeling budget on the simplified tasks (which all systems can perform). We assign an F1 score of 0 if a system fails to find a query in 1 hour. Across all labeling budgets tested, as above, PATSQL performs well when the target query is simplest (TQ1, 5, and 6). For other queries, PATSQL either fails

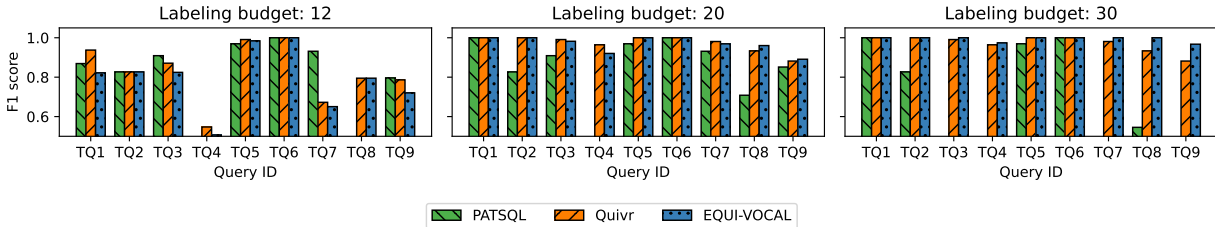


Figure 7: F1 score for queries without duration constraints on simplified tasks, under different user labeling budgets. PATSQL performs well only when the target query is simple. EQUI-VOCAL performs worse than Quivr when no additional examples are requested, but catches up and outperforms Quivr with a larger labeling budget.

Table 7: Probability that a system returns at least one query on noisy data. (false positive rate is 0.1 of false negative rate)

FN rate	0.1	0.2	0.3	0.4	0.5
Quivr, Mean	68%	54%	47%	34%	17%
(Range)	(20%-100%)	(35%-75%)	(5%-75%)	(5%-55%)	(0%-50%)
Ours, Mean	100%	100%	100%	100%	100%

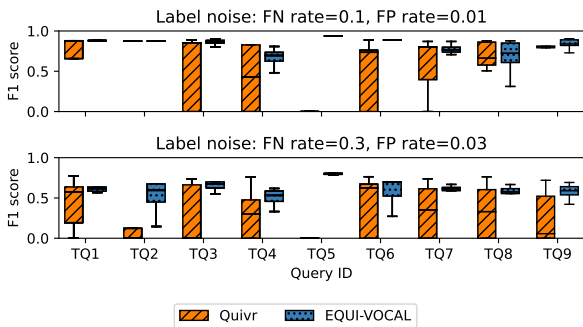


Figure 8: Impact of data noise, with a labeling budget of 20. EQUI-VOCAL constantly outperforms Quivr and is thus more robust to data noise.

to find a solution query within 1 hour or the solution query has low performance (below a 0.9 F1 score). When the budget is 30, we observe a decrease in F1 scores for TQ3, 7, 8, and 9, because PATSQL has a less constrained search space than EQUI-VOCAL and does not scale well when the size of input and output tables increases as more examples are provided. Quivr performs better than EQUI-VOCAL when no additional examples are requested (budget=12) because it enumerates the entire search space and finds all consistent queries using the initial examples, while EQUI-VOCAL prunes candidate queries at every iteration to ensure efficient query synthesis. With a larger labeling budget, EQUI-VOCAL can request more labels during the search process to select better paths to explore, thus it catches up with Quivr and outperforms it when the budget is 30.

EQUI-VOCAL is more robust to noisy data and produces higher quality queries than Quivr. We compare the performance of Quivr and EQUI-VOCAL when the data is noisy. We do not compare against PATSQL since its performance on video queries is already low even with perfect data. We inject noise into the original dataset by randomly flipping a fraction of the labels. We vary the false negative rate from 0.1 to 0.5 and set the false

Table 8: Number of queries explored and number of predictions per second to achieve at least 0.9 F1 scores. EQUI-VOCAL reduces computational effort by exploring fewer queries and by executing queries faster.

ID	# queries explored		ID	# predictions/s	
	Quivr	Ours		Quivr	Ours
TQ1	222748	1123	TQ1	154	574
TQ2	245112	1071	TQ2	124	666
TQ3	220627	1101	TQ3	140	664
TQ5	212066	1118	TQ5	140	480
TQ6	224504	1077	TQ6	151	547
TQ8	263040	1080	TQ8	145	792

positive rate to 0.1 the false negative one. Table 7 shows the percentage of runs when the system returned *any* queries for different noise rates. We evaluate the systems over 9 queries (TQ1-TQ9) in the simplified setting. For Quivr, we also report the range of the success rate besides the mean value. When the false negative rate is 0.1, Quivr has a 68% success rate, and this goes down to only 17% when the false negative rate is 0.5. In contrast, EQUI-VOCAL always returns k queries. To demonstrate that EQUI-VOCAL also produces higher quality queries, Figure 8 shows the F1 score of EQUI-VOCAL and Quivr with a labeling budget of 20, under two different noise rates. When Quivr fails to return any queries, we assign an F1 score of 0. EQUI-VOCAL performs better than Quivr for different queries and different noise rates.

EQUI-VOCAL is more computationally efficient than Quivr by exploring fewer queries and executing every query faster. Table 8 measures the number of queries explored and the number of predictions per second to achieve at least a 0.9 F1 score. We define a prediction as evaluating a query on a video segment, so the number of predictions per second reflects the efficiency of query execution. We evaluate over TQ1-TQ9 in the normal setting and report the numbers for queries that Quivr can synthesize. By limiting the query search to valid sequences of region graphs and by using the beam search strategy, the number of queries explored by EQUI-VOCAL is as small as 0.41% of Quivr. EQUI-VOCAL also executes queries faster than Quivr by up to 5.5 \times in terms of the number of predictions per second. These two factors together make EQUI-VOCAL more efficient than Quivr.

5.2 Results on scene graphs

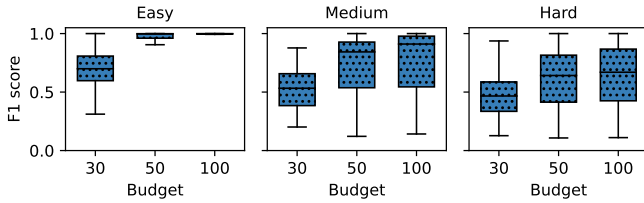


Figure 9: EQUI-VOCAL can synthesize high-quality queries within a reasonable budget, even for scene graph queries.

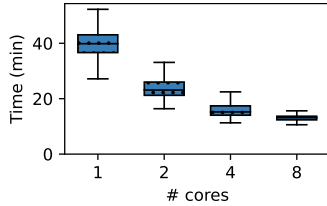


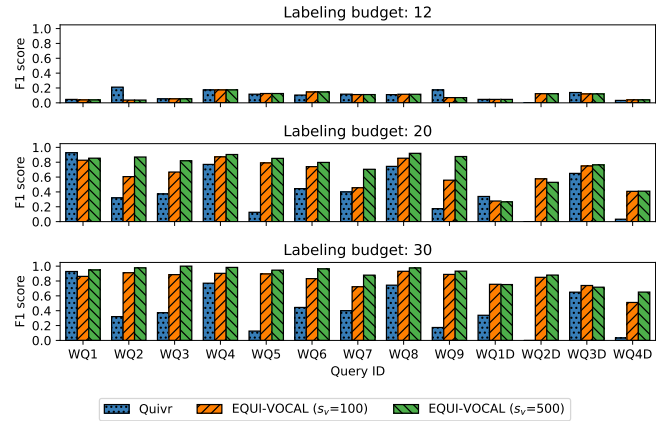
Figure 10: Vary # cores. EQUI-VOCAL can be easily parallelized to reduce synthesis time.

Next, we evaluate EQUI-VOCAL on the scene graphs dataset. Neither PATSQL nor Quivr support such flexible queries at video scale. Because the dataset is more complex, EQUI-VOCAL requires that the user provide a slightly larger (although still quite small) number of initial examples to avoid overfitting. We randomly select 15 positive and 15 negative examples from the training dataset as the initial examples. Later in Section 5.5, we discuss how varying the initial number of examples affects the system performance.

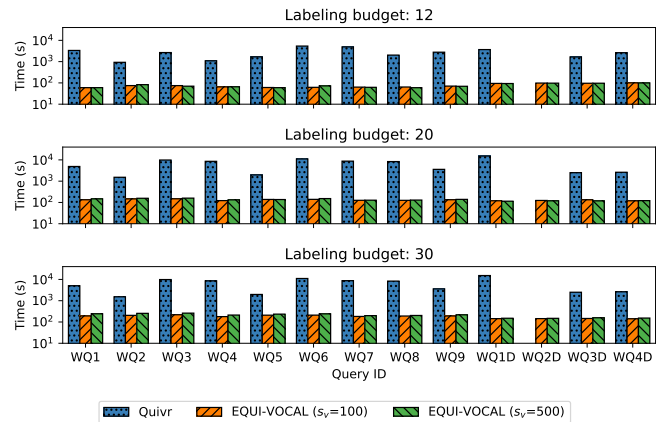
Figure 9 shows the F1 score of EQUI-VOCAL under different user labeling budgets. With a larger budget, EQUI-VOCAL can learn queries with higher F1 scores, and achieves a median F1 score of 1.0, 0.91, and 0.67 for easy, medium, and hard queries when the budget is 100. Results for a budget of 50 are nearly identical, which shows that **EQUI-VOCAL can synthesize high-quality queries within a reasonable budget, even for complex queries.**

EQUI-VOCAL does not learn good queries in all cases. We note that some queries are easier to synthesize than others, which results in the high variance of the F1 score in Figure 9. In particular, EQUI-VOCAL assumes that the ancestor queries of the target query are informative and leverages the performance of those queries to guide the search. However, if the ancestor queries cannot be distinguished from other queries in the same iteration (because they all have the same, typically low, F1 score), EQUI-VOCAL struggles with learning good queries. One direction of future work could explore other types of more fine-grained user feedback besides binary labels to help EQUI-VOCAL learn intermediate queries [65].

EQUI-VOCAL’s query synthesis time on the scene graphs dataset is greater than on the trajectories dataset. It increases from tens of seconds (Table 6) to minutes. **However, EQUI-VOCAL can easily be parallelized to reduce synthesis time, as executing queries in PostgreSQL is embarrassingly parallel.** Figure 10 shows the query synthesis time for the hard, scene-graphs queries when varying the number of cores and for a labeling budget of 50. Query synthesis time decreases significantly by using multiple cores



(a) F1 scores.



(b) Query synthesis time.

Figure 11: F1 scores and query synthesis time of EQUI-VOCAL and Quivr on the real-world dataset. EQUI-VOCAL can synthesize queries with high performance and is significantly faster than Quivr.

Table 9: Quivr’s success rate on the real-world dataset.

Query	WQ1	WQ4	WQ7	WQ8	WQ1D	WQ3D
Quivr success rate	40%	55%	35%	60%	5%	5%

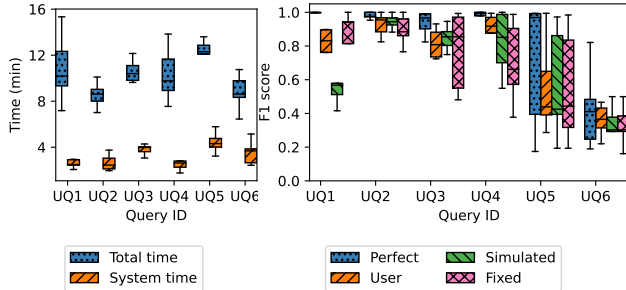
and reduces to 13 minutes with eight cores. EQUI-VOCAL achieves $1.76\times$ speedup with 2 cores and $3.03\times$ speedup with 8 cores. Note that this is the largest labeling budget for our experiments. With a lower budget, EQUI-VOCAL is even faster. The query synthesis time can be further reduced by using more cores, further decreasing the labeling budget, decreasing bw , or decreasing k .

5.3 Results on real-world dataset

We compare EQUI-VOCAL and Quivr on the real-world dataset and queries in Table 5. For WQ1-WQ9, we omit duration constraints from the search space. We randomly select 2 positive and 10 negative examples as initial examples. Since the target events are extremely rare in the dataset, we consider EQUI-VOCAL with two

Table 10: Queries used in the user study. “Pos %” is the percentage of positive examples in the dataset.

ID	Query	Description	Pos %
UQ1	(Color(o_1 , 'red'), Shape(o_2 , 'cylinder'), Far(o_1, o_2)); Near(o_1, o_2)	A red object is far from a cylinder, then they get close.	16.7%
UQ2	(Color(o_1 , 'purple'), Material(o_1 , 'metal'), Behind(o_1, o_2), Bottom(o_2))	A purple metal object o_1 is behind another object o_2 at the bottom of the screen.	24.2%
UQ3	(Color(o_1 , 'red'), Shape(o_2 , 'cylinder'), Far(o_1, o_2)); (Near(o_1, o_2), Top(o_3), Right(o_3))	A red object is far from a cylinder, then they get close while a third object is at the top right of the screen.	12.8%
UQ4	(Color(o_1 , 'purple'), Material(o_1 , 'metal'), Behind(o_1, o_2), Bottom(o_2)); Top(o_2)	A purple metal object o_1 is behind another object o_2 at the bottom of the screen, then o_2 moves to the top.	12.8%
UQ5	Duration((Color(o_1 , 'red'), Shape(o_2 , 'cylinder'), Far(o_1, o_2), 25); (Near(o_1, o_2), Top(o_3), Right(o_3)))	A red object is far from a cylinder for at least a second, then they are near each other while a third object is at the top right of the screen.	4.2%
UQ6	(Color(o_1 , 'purple'), Material(o_1 , 'metal'), Behind(o_1, o_2), Bottom(o_2)); Top(o_2); Duration((Bottom(o_3), Right(o_3)), 25)	A purple metal object o_1 is behind another object o_2 at the bottom of the screen, then o_2 moves to the top, then a third object o_3 is at the bottom right of the screen for at least a second.	3.8%

**(a) Task completion time.****(b) F1 score.****Figure 12: User study results. (a) Participants can complete the task in a reasonable amount of time. (b) For UQ1-UQ4, participants can help EQUI-VOCAL synthesize queries with at least 0.8 F1 scores.**

different s_v values, 100 and 500, to increase the number of sampled positive examples during active learning.

EQUI-VOCAL outperforms Quivr in terms of F1 scores and query synthesis time on the real-world dataset. Figure 11 shows the F1 score and query synthesis time of both systems under different labeling budgets. The timeout is set to 4 hours for both systems. EQUI-VOCAL can synthesize all queries in hundreds of seconds with a labeling budget of 30, while Quivr suffers from a low success rate (as shown in Table 9) and, even when it succeeds, takes thousands of seconds to synthesize queries. EQUI-VOCAL performs worse or similar to Quivr with a labeling budget of 12, but with some additional examples, EQUI-VOCAL can easily achieve higher F1 scores. In addition, sampling more candidate video segments during active learning ($s_v=500$) increases the F1 score in most cases but also slightly increases the synthesis time.

5.4 User study

We conduct a user study to understand the effectiveness and usability of EQUI-VOCAL. We use internal validation since asking participants to provide their own queries would make it difficult to compare across participants. Our goals include observing the system performance in the presence of user noise, measure task completion time, and collect qualitative feedback. We recruited 18 university students studying Computer Science. The study is conducted over the scene graphs dataset with six query tasks with different complexities, as shown in Table 10.

We started each session by explaining our definitions of predicates and walking through an example task with participants to get them familiar with the interface and the task. Each participant

Table 11: Labeling error rates of participants in the user study.

Error type	UQ1	UQ2	UQ3	UQ4	UQ5	UQ6
FP rate	0.250	0.065	0.169	0.028	0.308	0.029
FN rate	0.061	0.123	0.091	0.133	0.286	0.714

then completed three query tasks in sequence (either UQ1, 3, 5 or UQ2, 4, 6) with increasing complexity from easy, to medium, to hard. Each query task described the target complex event using natural language. In the user study, we provided the initial examples with ground-truth labels to EQUI-VOCAL so that participants could focus on interacting with the system during query synthesis. We randomly selected 10 positive and 10 negative examples for UQ1, 2 and 4 as the initial examples, and 15 for other queries to account for the increased query complexity. EQUI-VOCAL iteratively selected video segments to label, with a budget of 50 per task. After each task, participants reviewed the synthesized queries and provided subjective ratings and qualitative feedback via a questionnaire.

Participants are able to complete the task in a reasonable amount of time. Figure 12a shows the task completion time of each query. The median completion time of each task ranges between 8.6 and 12.3 minutes. The average time to label a video segment for each query task is 22, 16, 25, 20, 30, and 22 seconds, respectively. Also, the system time only takes a small portion of the total time, suggesting that EQUI-VOCAL is efficient.

EQUI-VOCAL is resilient to user noise, whereas Quivr is not. Figure 12b shows the F1 score of synthesized queries under different labeling scenarios: using the ground-truth labels (Perfect), using real user labels (User), using injected label noise with a false negative rate of 0.3 and a false positive rate of 0.03 (Fixed), and using injected label noise with the same noise rate as users for each query task (Simulated). Participants’ labeling error rates are shown in Table 11. Each experiment is run nine times. **F1 scores of User lie between Perfect and Simulated.** Due to the user noise, the query performance decreases compared to using perfect labels. Because the same error rate is used, Simulated’s performance is worse or similar to User’s, which justifies our expectations for the simulation experiment. **For queries that EQUI-VOCAL can synthesize with high quality, participants can help to find them with at least 0.8 F1 scores.** Not surprisingly, for queries (UQ5 & 6) that EQUI-VOCAL would fail even with perfect labels, participants cannot instruct the system to achieve better performance using the current prototype. Interestingly, most video segments that EQUI-VOCAL selects for hard queries are negative examples, making it difficult to learn good queries. However, these segments are not

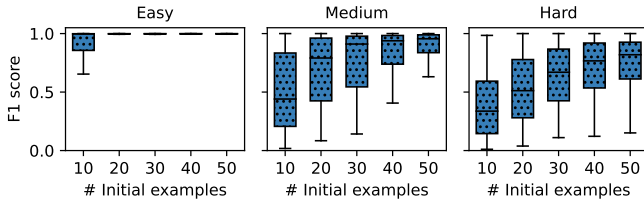


Figure 13: Providing more initial examples helps EQUI-VOCAL learn better queries and avoid overfitting.

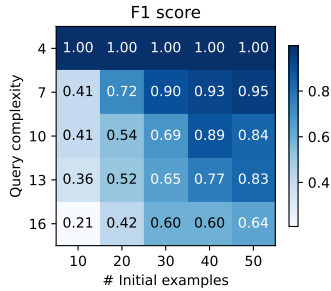


Figure 14: F1 score for various numbers of initial examples and queries with different complexity. EQUI-VOCAL obtains higher F1 scores with more initial examples and when the target queries are simpler.

equally negative, as many participants consider some negative samples to be almost positive that fail to satisfy one predicate. This suggests that EQUI-VOCAL could potentially benefit from more fine-grained user feedback.

Participants would like EQUI-VOCAL to be more responsive. In the questionnaire, the average rating of system responsiveness is 3.53 out of 5. Although the average system time across all tasks is only 195 seconds, participants observe greater latency in early and middle iterations, since there are more branches to expand and more candidate queries to evaluate. Taking UQ1 as an example, the average wait time to receive the first video segment in the 5th iteration is 31 seconds, while in the 10th iteration, it is only 1.3 seconds. Other techniques can be used to further hide the latency of the system [21], which is not the focus of this work.

5.5 Ablation study

We study the impact of hyperparameters and the sensitivity of EQUI-VOCAL to hyperparameter tuning. Unless otherwise specified, we evaluate EQUI-VOCAL on the scene graphs dataset and use the default values for hyperparameters that we are not studying.

EQUI-VOCAL synthesizes useful queries with a small number of initial examples, but providing more initial examples improves performance. Figure 13 shows EQUI-VOCAL’s F1 score for different numbers of initial examples, from five positives and five negatives (ten in total), to 25 positives and 25 negatives (50 in total), while the total labeling budget remains 100. When the number of initial examples is smallest, EQUI-VOCAL can incorrectly retain queries that overfit the examples in early iterations, leading to final results with low F1 scores. Results, however, quickly improve, and with as few as 30 initial examples, median F1 scores are high at 0.998, 0.911, and 0.670 for the easy, medium, and hard

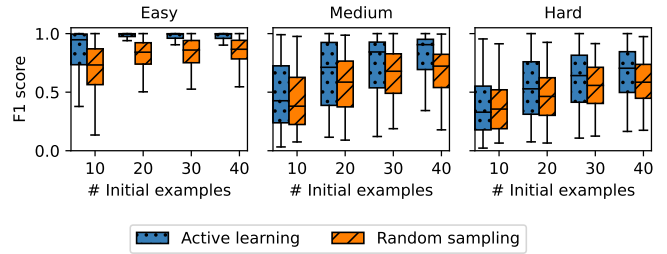


Figure 15: Active learning helps EQUI-VOCAL learn better queries compared to random sampling, and the improvement is more significant when the number of initial examples is larger.

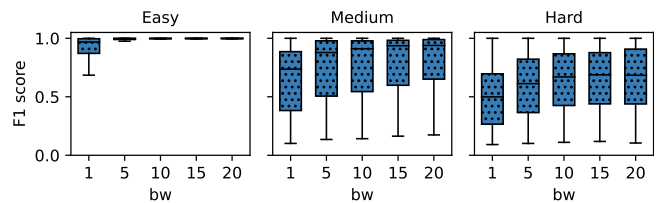


Figure 16: Increasing bw improves the performance of EQUI-VOCAL.

queries respectively. Figure 14 shows the F1 score of EQUI-VOCAL under different numbers of initial examples and queries with different complexity, while the total labeling budget remains 100. As expected, EQUI-VOCAL obtains higher F1 scores with more initial examples and when the target queries are simpler. The heatmap aggregates the results of all easy, medium, and hard queries, and we use $\alpha_1 = 1$, $\alpha_2 = 0.9$, $\alpha_3 = 0.2$ when computing the query complexity for better visualization. Because manually finding initial examples requires more user effort than labeling video segments selected by EQUI-VOCAL, our approach is to balance user effort and system’s performance, using 30 initial examples in all other experiments on the scene graphs dataset. Interestingly, since EQUI-VOCAL can produce good queries in many cases even with a few examples, users always have the option to first start with a small set and restart with more examples if needed.

Active learning helps EQUI-VOCAL learn better queries quicker than randomly sampling video segments to label. Figure 15 shows EQUI-VOCAL’s F1 score when either using active learning or randomly selecting additional examples during query synthesis. We set the labeling budget to 50, and we vary the number of initial examples. The improvement of active learning over random sampling is more significant when the number of initial examples is larger since fewer labels are requested per iteration and the selection of informative examples becomes more important.

Increasing the beam width improves performance, but also increases the synthesis time. Figure 16 shows the F1 score of EQUI-VOCAL under different values of bw . Increasing bw from 1 to 10 increases median F1 scores on easy queries by 3.10%, on medium queries by 23.8%, and on hard queries by 34.3%, but increasing from 10 to 20 only further improves median scores by up to 3.07%. At the same time, increasing bw from 10 to 15 increases the median synthesis time on hard queries by 27.8%. EQUI-VOCAL

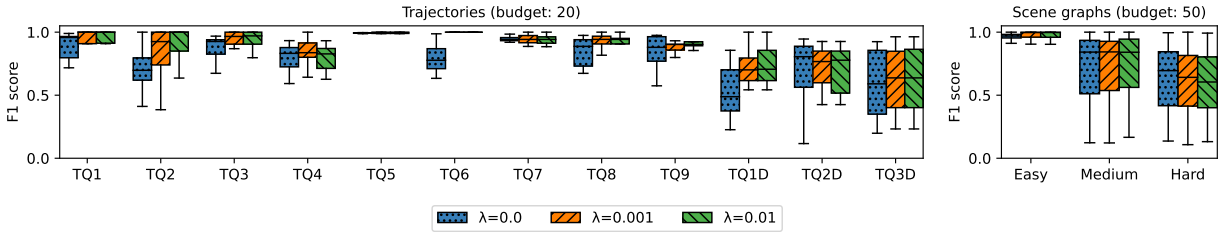


Figure 17: Regularization ($\lambda = 0.001$ and $\lambda = 0.01$) helps EQUI-VOCAL to learn better queries in many cases and does not harm the performance in other cases.

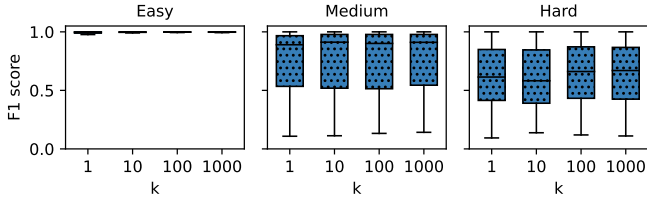


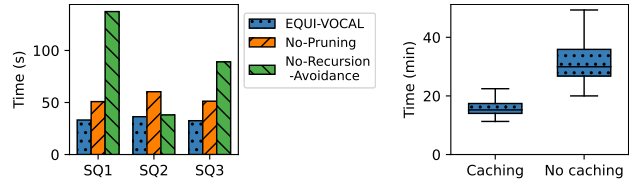
Figure 18: Increasing k slightly improves the performance of EQUI-VOCAL.

defaults to $bw = 10$ to strike a balance between query performance and synthesis time.

Regularization helps EQUI-VOCAL learn better queries in many cases and does not harm performance in other cases. Figure 17 shows the F1 score of EQUI-VOCAL on both the trajectories dataset and the scene graphs dataset, under different values of λ . For the trajectory pairs dataset, we set the labeling budget to 20 and the initial number of examples to 12 (i.e., two positive and ten negative examples); for the scene graphs dataset, we set the labeling budget to 50 and the initial number of examples to 30. For the trajectories dataset, we see an improvement for many queries with regularization, especially when the queries are simple (e.g., with fewer predicates). With $\lambda = 0.01$, we see a median improvement between 44.6% and -3.44% for the queries from Table 3. TQ4, TQ9, TQ2D, and TQ3D are more complex than other queries and have four predicates, so applying regularization is unlikely to improve the performance. For the more complex scene graphs dataset, regularization does not improve F1 scores but also does not compromise system performance. With $\lambda = 0.001$, the median change in F1 score stays between 2.84% and -7.69% . For this reason, EQUI-VOCAL defaults to using a small regularization factor.

increasing k slightly improves performance. We evaluate the F1 score of EQUI-VOCAL under different values of k , as shown in Figure 18. For medium and hard scene graph queries, increasing k from 1 to 1000 slightly improves the median F1 score by 2.36% and 9.12% respectively. Since the target queries are complex, they are not explored until later iterations of the algorithm, when most labeling budget has been used. Labels requested afterward have little impact on the ranking of the queries in the list, so the performance improvement from increasing k is also limited. Easy queries already have near-perfect F1 scores, so increasing k does not improve performance.

EQUI-VOCAL’s query execution optimizations significantly reduce query synthesis times. Figure 19a shows the average query execution time for variants of our query translation



(a) Single query execution time with different SQL optimizations.

(b) Synthesis time with and without caching.

Figure 19: Impact of query execution optimizations. EQUI-VOCAL reduces query synthesis time by (a) generating efficient SQL queries that prune intermediate results and avoid recursion, and (b) using a caching mechanism.

Table 12: Median F1 scores of EQUI-VOCAL and ML methods. EQUI-VOCAL achieves higher F1 scores for all queries.

Queries	Ours	CLIP	MViT	CLIP (all)	MViT (all)
Easy	0.997	0.249	0.222	0.327	0.322
Medium	0.843	0.201	0.182	0.278	0.255
Hard	0.638	0.219	0.203	0.286	0.265

algorithm on scene graph queries. We generate SQL queries using our complete query translation algorithm, and two variants that omit optimizations of pruning intermediate results and avoiding recursion, respectively, and then execute them over all 10,000 video segments from the scene graphs dataset in PostgreSQL. We evaluate EQUI-VOCAL on SQ1-SQ3, and each query is executed 20 times. As the figure shows, the query execution time increases dramatically without either optimization. Pruning intermediate results boosts performance by up to 1.66 \times . Recursion avoidance is important when the query contains duration constraints (SQ1 and SQ3), providing up to a 4.14 \times speedup.

Figure 19b shows the impact of our caching mechanism. Caching query results leads to a 1.97 \times speedup. We experimented on hard queries using four CPUs and a labeling budget of 50.

5.6 Comparing with machine learning method

To determine whether a video segment contains an event of interest, EQUI-VOCAL’s query synthesis approach could be substituted by training an ML model. However, this approach requires a large number of labeled examples and complicates interpretability [23]. We compare EQUI-VOCAL against an existing ML approach that builds domain-specific models for videos [21] on the scene graphs dataset.

For EQUI-VOCAL, we adopt the same setting as outlined in Section 5.2, with a labeling budget of 50. The ML approach extracts features using pretrained video and image models and trains a linear model using the same set of user-labeled video segments selected by EQUI-VOCAL. We use both MVIT [22] and CLIP [60] as the feature extractors. Table 12 shows that **EQUI-VOCAL achieves higher F1 scores than the ML approach for all queries, even when using CLIP with all 500 training samples.**

6 RELATED WORK

Video analytics systems. Many recent VDBMSs have been proposed and focus on a wide range of data management challenges, including fast inference over videos [4, 6, 40, 52, 56], storage optimization [19, 28, 79], efficient dataflow processing [58], preprocessing and indexing [7, 33, 42], exploration and organization [20], privacy [10], and tuning configurations [34, 38, 63]. Those techniques are orthogonal to our work.

Compositional query processing over videos. Several systems have explored compositional queries over videos [8, 12, 15–18, 24, 46, 50, 55, 80]. However, they either require that users express compositional queries explicitly [15, 24, 50], or train customized models for such events [8, 12, 18]. Instead, EQUI-VOCAL uses a query-by-example approach to minimize user effort and learn and refine a query specification iteratively from user feedback.

Accelerating query execution over visual data. Prior work has focused on accelerating queries by pre-filtering frames to avoid expensive computation [30, 31, 52], optimizing the sampling rate [6, 56], and building specialized models [4, 40]. EQUI-VOCAL currently extracts all objects in a video before the search process, but could leverage those existing techniques to avoid running expensive object detection and tracking algorithms on all frames.

Query by example. Many systems have been proposed for SQL queries over relational data [23, 49, 59, 70, 73]. EQUI-VOCAL focuses on learning queries for video events, with a more constrained form than general relational queries. Quivr [55] is most similar to our work, but it only operates over object trajectories and assumes noiseless inputs. SQuID [23] synthesizes queries based on semantic similarity but does not support self-joins and non-equi joins, which are necessary to find our video events, and S4 [59] ranks queries based on input containment and is limited to project-join queries.

Program synthesis. Program synthesis has been used for a wide range of tasks, such as generating referring relational programs [35], authoring visualizations [74], learning relational data transformation [39], and synthesizing programs for string processing [57]. Unlike these systems, EQUI-VOCAL synthesizes queries in the domain of videos, which is significantly different in terms of the spatio-temporal complexity and the prevalence of noise.

Active learning. Model Picker [43] uses active learning to distinguish the best model from a set of pretrained classifiers. EQUI-VOCAL adapts this approach to select the most promising queries to explore. Quivr [55] also prunes candidate queries using active learning, but only after enumerating all candidates. In contrast, EQUI-VOCAL integrates active learning and labeling into the search process to expand only the most promising queries in each iteration, ensuring both synthesis efficiency and query performance.

7 CONCLUSION

In this paper, we presented EQUI-VOCAL, a new system that synthesizes compositional queries from examples. EQUI-VOCAL models compositional events as spatio-temporal scene graphs, explores the query search space using results of executing intermediate queries and beam search, leverages active learning to reduce user effort, and generates efficient SQL queries to reduce computational effort.

ACKNOWLEDGMENTS

This work was supported in part by the NSF through awards CCF-1703051 and IIS-2211133 as well as a grant from CISCO.

REFERENCES

- [1] 2022. EQUI-VOCAL. <https://github.com/uwdb/EQUI-VOCAL>.
- [2] Sherif M. Abdou and Michael S. Scordilis. 2004. Beam search pruning in speech recognition using a posterior probability-based confidence measure. *Speech Commun.* 42, 3-4 (2004), 409–428.
- [3] Ganesh Ananthanarayanan, Paramvir Bahl, Peter Bodik, Krishna Chintalapudi, Matthai Philipose, Lenin Ravindranath, and Sudipta Sinha. 2017. Real-Time Video Analytics: The Killer App for Edge Computing. *Computer* 50, 10 (2017), 58–67.
- [4] Michael R. Anderson, Michael J. Cafarella, Germán Ros, and Thomas F. Wenisch. 2019. Physical Representation-Based Predicate Optimization for a Visual Analytics Database. In *ICDE*. 1466–1477.
- [5] Emmanouil N Barmounakis, Eleni I Vlahogianni, and John C Golias. 2016. Unmanned Aerial Aircraft Systems for transportation engineering: Current practice and future challenges. *IJTST* 5, 3 (2016), 111–122.
- [6] Favyen Bastani, Songtao He, Arjun Balasingam, Karthik Gopalakrishnan, Mohammad Alizadeh, Hari Balakrishnan, Michael J. Cafarella, Tim Kraska, and Sam Madden. 2020. MIRIS: Fast Object Track Queries in Video. In *SIGMOD*. 1907–1921.
- [7] Favyen Bastani and Samuel Madden. 2022. OTIF: Efficient Tracker Pre-processing over Large Video Datasets. In *SIGMOD*. 2091–2104.
- [8] Favyen Bastani, Oscar R. Moll, and Samuel Madden. 2020. Vaas: Video Analytics At Scale. *PVLDB* 13, 12 (2020), 2877–2880.
- [9] Irving Biederman. 1987. Recognition-by-components: a theory of human image understanding. *Psychological review* 94, 2 (1987), 115.
- [10] Frank Cangialosi, Neil Agarwal, Venkat Arun, Srinivas Narayana, Anand D. Sarwate, and Ravi Netravali. 2022. Privid: Practical, Privacy-Preserving Video Analytics Queries. In *NSDI*. 209–228.
- [11] Shih-Fu Chang, William Chen, Horace J. Meng, Hari Sundaram, and Di Zhong. 1997. VideoQ: An Automated Content Based Video Search System Using Visual Cues. In *MM*. 313–324.
- [12] Daren Chao, Nick Koudas, and Ioannis Xarchakos. 2020. SVQ++: Querying for Object Interactions in Video Streams. In *SIGMOD*. 2769–2772.
- [13] Vincent S. Chen, Paroma Varma, Ranjay Krishna, Michael S. Bernstein, Christopher Ré, and Li Fei-Fei. 2019. Scene Graph Prediction With Limited Labels. *ICCV* (2019).
- [14] Xinyun Chen, Chang Liu, and Dawn Song. 2019. Execution-Guided Neural Program Synthesis. In *ICLR*.
- [15] Yueting Chen, Nick Koudas, Xiaohui Yu, and Ziqiang Yu. 2022. Spatial and Temporal Constrained Ranked Retrieval over Videos. *PVLDB* 15, 11 (2022), 3226–3239.
- [16] Yueting Chen, Xiaohui Yu, and Nick Koudas. 2020. TQVS: Temporal Queries over Video Streams in Action. In *SIGMOD*. 2737–2740.
- [17] Yueting Chen, Xiaohui Yu, Nick Koudas, and Ziqiang Yu. 2021. Evaluating Temporal Queries Over Video Feeds. In *SIGMOD*. 287–299.
- [18] Pramod Chunduri, Jaeho Bang, Yao Lu, and Joy Arulraj. 2022. Zeus: Efficiently Localizing Actions in Videos using Reinforcement Learning. In *SIGMOD*. 545–558.
- [19] Maureen Daum, Brandon Haynes, Dong He, Amrita Mazumdar, and Magdalena Balazinska. 2021. TASM: A Tile-Based Storage Manager for Video Analytics. In *ICDE*. 1775–1786.
- [20] Maureen Daum, Enhao Zhang, Dong He, Magdalena Balazinska, Brandon Haynes, Ranjay Krishna, Apryle Craig, and Aaron Wirsing. 2022. VOCAL: Video Organization and Interactive Compositional Analytics. In *CIDR*.
- [21] Maureen Daum, Enhao Zhang, Dong He, Stephen Mussmann, Brandon Haynes, Ranjay Krishna, and Magdalena Balazinska. 2023. VOCALExplorer: Pay-as-You-Go Video Data Exploration and Model Building. *arXiv preprint arXiv:2303.04068* (2023).
- [22] Haoqi Fan, Bo Xiong, Karttikeya Mangalam, Yanghao Li, Zhicheng Yan, Jitendra Malik, and Christoph Feichtenhofer. 2021. Multiscale Vision Transformers. In *ICCV*. IEEE, 6804–6815.

- [23] Anna Fariha and Alexandra Meliou. 2019. Example-Driven Query Intent Discovery: Abductive Reasoning using Semantic Similarity. *PVLDB* 12, 11 (2019), 1262–1275.
- [24] Daniel Y. Fu, Will Crichton, James Hong, Xinwei Yao, Haotian Zhang, Anh Truong, Avanika Narayan, Maneesh Agrawala, Christopher Ré, and Kayvon Fatahalian. 2019. Recall: Specifying Video Events using Compositions of Spatiotemporal Labels. *arXiv preprint arXiv:1910.02993* (2019).
- [25] Andreas Geiger, Philip Lenz, and Raquel Urtasun. 2012. Are we ready for autonomous driving? the kitti vision benchmark suite. In *CVPR*. 3354–3361.
- [26] Shilpa George, Junjue Wang, Mihir Bala, Thomas Eiszler, Padmanabhan Pillai, and Mahadev Satyanarayanan. 2019. Towards Drone-sourced Live Video Analytics for the Construction Industry. In *HotMobile*. 3–8.
- [27] Patrick Hammer, Tony Lofthouse, Enzo Fenoglio, Hugo Latapie, and Pei Wang. 2020. A Reasoning Based Model for Anomaly Detection in the Smart City Domain. In *IntelliSys (AISC)*, Vol. 1251. 144–159.
- [28] Brandon Haynes, Maureen Daum, Dong He, Amrita Mazumdar, Magdalena Balazinska, Alvin Cheung, and Luis Ceze. 2021. VSS: A Storage System for Video Analytics. In *SIGMOD*. 685–696.
- [29] Brandon Haynes, Amrita Mazumdar, Magdalena Balazinska, Luis Ceze, and Alvin Cheung. 2019. Visual Road: A Video Data Management Benchmark. In *SIGMOD*. 972–987.
- [30] Dong He, Maureen Daum, Walter Cai, and Magdalena Balazinska. 2021. DeepEverest: Accelerating Declarative Top-K Queries for Deep Neural Network Interpretation. *PVLDB* 15, 1 (2021), 98–111.
- [31] Dong He, Jieyu Zhang, Maureen Daum, Alexander Ratner, and Magdalena Balazinska. 2023. MaskSearch: Querying Image Masks at Scale. *arXiv preprint arXiv:2305.02375* (2023).
- [32] Kaiming He, Georgia Gkioxari, Piotr Dollár, and Ross B. Girshick. 2017. Mask R-CNN. In *ICCV*. 2980–2988.
- [33] Wenjia He, Michael R. Anderson, Maxwell Strome, and Michael J. Cafarella. 2020. A Method for Optimizing Opaque Filter Queries. In *SIGMOD*. 1257–1272.
- [34] Wenjia He and Michael J. Cafarella. 2022. Controlled Intentional Degradation in Analytical Video Systems. In *SIGMOD*. 2105–2119.
- [35] Jiani Huang, Calvin Smith, Osbert Bastani, Rishabh Singh, Aws Albarghouthi, and Mayur Naik. 2020. Generating Programmatic Referring Expressions via Program Synthesis. In *ICML*, Vol. 119. 4495–4506.
- [36] Jingwei Ji, Ranjay Krishna, Li Fei-Fei, and Juan Carlos Niebles. 2020. Action genome: Actions as compositions of spatio-temporal scene graphs. In *CVPR*. 10236–10247.
- [37] Ruyi Ji, Jingjing Liang, Yingfei Xiong, Lu Zhang, and Zhenjiang Hu. 2020. Question selection for interactive program synthesis. *Proceedings of the 41st ACM SIGPLAN Conference on Programming Language Design and Implementation* (2020).
- [38] Junchen Jiang, Ganesh Ananthanarayanan, Peter Bodik, Siddhartha Sen, and Ion Stoica. 2018. Chameleon: scalable adaptation of video analytics. In *SIGCOMM*. 253–266.
- [39] Sean Kandel, Andreas Paepcke, Joseph M. Hellerstein, and Jeffrey Heer. 2011. Wrangler: interactive visual specification of data transformation scripts. In *CHI*. 3363–3372.
- [40] Daniel Kang, Peter Bailis, and Matei Zaharia. 2019. Blazelt: Optimizing Declarative Aggregation and Limit Queries for Neural Network-Based Video Analytics. *PVLDB* 13, 4 (2019), 533–546.
- [41] Daniel Kang, John Emmons, Firas Abuzaid, Peter Bailis, and Matei Zaharia. 2017. NoScope: Optimizing Deep CNN-Based Queries over Video Streams at Scale. *PVLDB* 10, 11 (2017), 1586–1597.
- [42] Daniel Kang, John Guibas, Peter D. Bailis, Tatsunori Hashimoto, and Matei Zaharia. 2022. TASTI: Semantic Indexes for Machine Learning-based Queries over Unstructured Data. In *SIGMOD*. 1934–1947.
- [43] Mohammad Reza Karimi, Nezih Merve Gürel, Bojan Karlas, Johannes Rausch, Ce Zhang, and Andreas Krause. 2021. Online Active Model Selection for Pre-trained Classifiers. In *AISTATS*, Vol. 130. 307–315.
- [44] Ranjay Krishna, Yuke Zhu, Oliver Groth, Justin Johnson, Kenji Hata, Joshua Kravitz, Stephanie Chen, Yannis Kalantidis, Li-Jia Li, David A. Shamma, Michael S. Bernstein, and Li Fei-Fei. 2017. Visual Genome: Connecting Language and Vision Using Crowdsourced Dense Image Annotations. *IJCV* 123, 1 (2017), 32–73.
- [45] Abhishek Kumar, Shankar Vembu, Aditya Krishna Menon, and Charles Elkan. 2013. Beam search algorithms for multilabel learning. *Mach. Learn.* 92, 1 (2013), 65–89.
- [46] Tony C. T. Kuo and Arbee L. P. Chen. 2000. Content-Based Query Processing for Video Databases. *TMM* 2, 1 (2000), 1–13.
- [47] Christopher A Kurby and Jeffrey M Zacks. 2008. Segmentation in the perception and memory of events. *Tics* 12, 2 (2008), 72–79.
- [48] David D. Lewis and Jason Catlett. 1994. Heterogeneous Uncertainty Sampling for Supervised Learning. In *ICML*.
- [49] Hao Li, Chee-Yong Chan, and David Maier. 2015. Query From Examples: An Iterative, Data-Driven Approach to Query Construction. *PVLDB* 8, 13 (2015), 2158–2169.
- [50] Xiao Chen Liu, Pradipta Ghosh, Oytun Ulutan, B. S. Manjunath, Kevin S. Chan, and Ramesh Govindan. 2019. Caesar: cross-camera complex activity recognition. In *SenSys*. 232–244.
- [51] Ximing Lu, Sean Welleck, Peter West, Liwei Jiang, Jungo Kasai, Daniel Khashabi, Ronan Le Bras, Lianhui Qin, Youngjae Yu, Rowan Zellers, Noah A. Smith, and Yejin Choi. 2022. NeuroLogic A²esque Decoding: Constrained Text Generation with Lookahead Heuristics. In *NAACL*. 780–799.
- [52] Yao Lu, Aakanksha Chowdhery, Srikanth Kandula, and Surajit Chaudhuri. 2018. Accelerating Machine Learning Inference with Probabilistic Predicates. In *SIGMOD*. 1493–1508.
- [53] Rachael Mady, Peter Mason, Matt Strimas-Mackey, Miyoko Chu, Tina Phillips, David Bonter, Charles Eldermire, and Benjamin Walters. 2021. Bird Cams Lab Biological Data. <https://ecommons.cornell.edu/handle/1813/110264>.
- [54] Clara Meister, Ryan Cotterell, and Tim Vieira. 2020. Best-First Beam Search. *Trans. Assoc. Comput. Linguistics* 8 (2020), 795–809.
- [55] Stephen Mell, Favyen Bastani, Stephan Zdancewic, and Osbert Bastani. 2021. Synthesizing Video Trajectory Queries. In *AIPANS Workshop*.
- [56] Oscar Moll, Favyen Bastani, Sam Madden, Michael Stonebraker, Vijay N. Gadeppally, and Tim Kraska. 2020. ExSample: Efficient Searches on Video Repositories through Adaptive Sampling. *ICDE* (2020), 3065–3077.
- [57] Augustus Odena, Kensen Shi, David Bieber, Rishabh Singh, Charles Sutton, and Hanjun Dai. 2021. BUSTLE: Bottom-Up Program Synthesis Through Learning-Guided Exploration. In *ICLR*.
- [58] Alex Poms, Will Crichton, Pat Hanrahan, and Kayvon Fatahalian. 2018. Scanner: Efficient Video Analysis at Scale. *ACM Trans. Graph.* 37, 4 (2018).
- [59] Fotis Psallidas, Bolin Ding, Kaushik Chakrabarti, and Surajit Chaudhuri. 2015. S4: Top-k Spreadsheet-Style Search for Query Discovery. In *SIGMOD*. 2001–2016.
- [60] Alec Radford, Jong Wook Kim, Chris Hallacy, Aditya Ramesh, Gabriel Goh, Sandhini Agarwal, Girish Sastry, Amanda Askell, Pamela Mishkin, Jack Clark, Gretchen Krueger, and Ilya Sutskever. 2021. Learning Transferable Visual Models From Natural Language Supervision. In *ICML*, Vol. 139. PMLR, 8748–8763.
- [61] Veselin Raychev, Pavol Bielik, Martin T. Vechev, and Andreas Krause. 2016. Learning programs from noisy data. In *POPL*. 761–774.
- [62] Shaoqing Ren, Kaiming He, Ross B. Girshick, and Jian Sun. 2015. Faster R-CNN: Towards Real-Time Object Detection with Region Proposal Networks. In *NeurIPS*. 91–99.
- [63] Francisco Romero, Mark Zhao, Neeraja J. Yadwadkar, and Christos Kozyrakis. 2021. Llama: A Heterogeneous & Serverless Framework for Auto-Tuning Video Analytics Pipelines. In *SoCC*. 1–17.
- [64] Nicholas Roy and Andrew McCallum. 2001. Toward Optimal Active Learning through Sampling Estimation of Error Reduction. In *ICML*.
- [65] Olga Russakovsky, Li-Jia Li, and Li Fei-Fei. 2015. Best of both worlds: Human-machine collaboration for object annotation. In *CVPR*. 2121–2131.
- [66] Ozan Sener and Silvio Savarese. 2018. Active Learning for Convolutional Neural Networks: A Core-Set Approach. In *ICLR*.
- [67] Andrew W Senior, L Brown, Arun Hampapur, C-F Shu, Yun Zhai, Rogério Schmidt Feris, Y-L Tian, Sergio Borger, and C Carlson. 2007. Video analytics for retail. In *AVSS*. 423–428.
- [68] H. Sebastian Seung, Manfred Opper, and Haim Sompolinsky. 1992. Query by committee. In *Annual Conference Computational Learning Theory*.
- [69] Manuel Stein, Halldor Janetzko, Andreas Lamprecht, Thorsten Breitzkreutz, Philipp Zimmermann, Bastian Goldlücke, Tobias Schreck, Gennady L. Andrienko, Michael Grossniklaus, and Daniel A. Keim. 2018. Bring It to the Pitch: Combining Video and Movement Data to Enhance Team Sport Analysis. *TVCG* 24, 1 (2018), 13–22.
- [70] Keita Takenouchi, Takashi Ishio, Joji Okada, and Yuji Sakata. 2021. PATSQL: Efficient Synthesis of SQL Queries from Example Tables with Quick Inference of Projected Columns. *PVLDB* 14, 11 (2021), 1937–1949.
- [71] Abhishek Udupa, Arun Raghavan, Jyotirmoy V. Deshmukh, Sela Mador-Haim, Milo M. K. Martin, and Rajeev Alur. 2013. TRANSIT: specifying protocols with concolic snippets. In *PLDI*. 287–296.
- [72] Ashwin K Vijayakumar, Michael Cogswell, Ramprasad R Selvaraju, Qing Sun, Stefan Lee, David Crandall, and Dhruv Batra. 2016. Diverse beam search: Decoding diverse solutions from neural sequence models. *arXiv preprint arXiv:1610.02424* (2016).
- [73] Chenglong Wang, Alvin Cheung, and Rastislav Bodik. 2017. Synthesizing highly expressive SQL queries from input-output examples. *PLDI* (2017).
- [74] Chenglong Wang, Yu Feng, Rastislav Bodik, Isil Dillig, Alvin Cheung, and Amy J. Ko. 2021. Falx: Synthesis-Powered Visualization Authoring. In *CHI*. 106:1–106:15.
- [75] Junjue Wang, Ziqiang Feng, Zhuo Chen, Shilpa George, Mihir Bala, Padmanabhan Pillai, Shao-Wen Yang, and Mahadev Satyanarayanan. 2018. Bandwidth-Efficient Live Video Analytics for Drones Via Edge Computing. In *SEC*. 159–173.
- [76] Sida I. Wang, Samuel Ginn, Percy Liang, and Christopher D. Manning. 2017. Naturalizing a Programming Language via Interactive Learning. In *ACL*. 929–938.
- [77] Xiaoli Wang, Aakanksha Chowdhery, and Mung Chiang. 2016. SkyEyes: adaptive video streaming from UAVs. In *HotWireless*. 2–6.
- [78] Nicolai Wojke and Alex Bewley. 2018. Deep Cosine Metric Learning for Person Re-identification. In *WACV*. 748–756.

- [79] Tiantu Xu, Luis Materon Botelho, and Felix Xiaozhu Lin. 2019. VStore: A Data Store for Analytics on Large Videos. In *EuroSys*. 16:1–16:17.
- [80] Piyush Yadav and Edward Curry. 2019. VidCEP: Complex Event Processing Framework to Detect Spatiotemporal Patterns in Video Streams. In *Big Data*. 2513–2522.
- [81] Kexin Yi, Chuang Gan, Yunzhu Li, Pushmeet Kohli, Jiajun Wu, Antonio Torralba, and Joshua B. Tenenbaum. 2020. CLEVRER: Collision Events for Video Representation and Reasoning. In *ICLR*.
- [82] Quanzeng You, Hailin Jin, Zhaowen Wang, Chen Fang, and Jiebo Luo. 2016. Image Captioning with Semantic Attention. In *CVPR*. 4651–4659.
- [83] Jeffrey M Zacks, Barbara Tversky, and Gowri Iyer. 2001. Perceiving, remembering, and communicating structure in events. *Journal of experimental psychology: General* 130, 1 (2001), 29.
- [84] Jingwei Zhuo, Ziru Xu, Wei Dai, Han Zhu, Han Li, Jian Xu, and Kun Gai. 2020. Learning Optimal Tree Models under Beam Search. In *ICML*. 11650–11659.